Renewable Energy 249 (2025) 123215

Contents lists available at ScienceDirect

Renewable Energy

journal homepage: www.elsevier.com/locate/renene

Deep eutectic solvent pre-treatment of residual biomass streams – Effects on anaerobic degradability

Jana Schultz [a,*], Asli Isci [b], Marvin Scherzinger [a], Simel Bagder Elmaci [b], Miyase Deniz Cam [b], Dicle Delal Aslanhan [b], Ozge Sakiyan [b], Martin Kaltschmitt [a]

[a] Hamburg University of Technology (TUHH), Institute of Environmental Technology and Energy Economics (IUE), Eißendorfer Str. 40, 21073, Hamburg, Germany
[b] Ankara University, Food Engineering Department, 06830, Golbasi, Ankara, Turkey

ARTICLE INFO

Keywords:
Biogas
Anaerobic digestion
Pre-treatment
Deep eutectic solvents
Agricultural residues
Lignocellulosic biomass

ABSTRACT

The suitability of residual biomass from biorefineries as biogas substrate, including the effect of DES pre-treatment on biogas potential and biomass composition was evaluated. Three different biomasses, i.e., cork dust, olive tree pruning, and common reed, were treated with a deep eutectic solvent (DES; i.e., choline chloride and formic acid, 1:2 M ratio, 1:10 (g mL^{-1}) solid to solvent ratio) under various conditions. While being ineffective under less severe conditions, significantly increased biogas potentials were observed for all biomasses at 130 °C and 40 and/or 60 min of pre-treatment. Cork dust had the highest relative increase in biogas potential of 125 % (130 °C, 60 min). With an increase of 90 $mL_N\ g_{VS}^{-1}$ (+21 %), olive tree pruning showed the highest absolute increase. Common reed demonstrated a notable increase of 12 %. Concurrently, kinetic modelling revealed shifts in degradation kinetics, such as altered lag phases and higher maximum biogas rates, hereby the Cone Model provided the best fit for the data. The change could be attributed to delignification and retention of the fermentable glucan fraction in the solid biomass. Despite considerable differences among the biomasses, the results underscore the efficacy of DES pre-treatment in enhancing the anaerobic degradability of residual biomass.

List of abbreviations and nomenclature

a	Absorbance
ChCl	Choline chloride
CL	Cellulose to lignin ratio (–)
CR	Crystallinity ratio (–)
DM	Dry mass content (%)
DES	Deep eutectic solvent
e	Euler's number (2.7182)
FA	Formic acid
HBA	hydrogen bond acceptor
HBD	hydrogen bond donor
k_h	Rate constant (d^{-1})
LR	Lignin removal rate (%)
λ	Lag phase (d)
m	Mass (g)
m_0	Mass of sample before treatment (g)
m_a	Mass of the ash (g)
m_d	Mass of the dry sample (g)
m_f	Mass of the fresh sample (g)
m_t	Mass of sample after treatment (g)

(continued on next column)

(*continued*)

p	Pressure (hPa)
p_N	Normal pressure (1013 hPa)
p_w	Water vapor pressure (hPa)
P	Cumulative biogas production at time t ($mL_N\ g_{VS}^{-1}$)
P_0	Maximum biogas yield ($mL_N\ g_{VS}^{-1}$)
R^2	Coefficient of determination (–)
R_m	Maximum biogas production rate ($mL_N\ g_{VS}^{-1}\ d^{-1}$)
$RMSE$	Root mean square error ($mL_N\ g_{VS}^{-1}$)
ρ_{CH4}	Density of methane at 20 °C, atm. pressure (0.659 kg m^{-3})
s	Shape factor (–)
SSR	Solid to solvent ratio
SR	Solid recovery (%)
T	Temperature (°C)
t	Time (d)
T_N	Normal temperature (273 K)
V	Volume (mL)
$V_{dry,N}$	Volume of dry gas in normal state (mL_N)
VS	Volatile solids (%)
Y_{BG}	Biogas potential ($mL_N\ g_{VS}^{-1}$)

* Corresponding author.
E-mail address: jana.schultz@tuhh.de (J. Schultz).

https://doi.org/10.1016/j.renene.2025.123215
Received 22 July 2024; Received in revised form 16 April 2025; Accepted 18 April 2025
Available online 19 April 2025

1. Introduction

Biogas plants represent a mature technology for the provision of renewable heat and power, which could play a crucial role in the ongoing energy transition towards a fossil-free and more climate-friendly energy system. Beyond that, biogas plants may promote circularity in agriculture, allowing for effective waste management of organic residues and functioning as fertilizer production units. Moreover, they could serve as key units in modern biorefineries [1].

In the context of biorefineries, the production of biobased value-added products is typically prioritized over an energetic utilization – often due to economic considerations [1]. Nevertheless, the production of bioenergy in the form of biogas from organic process residuals and organic waste streams through anaerobic digestion, being typically the final sink for all types of biogenic residues, remains a key element of circular approaches. The selection of substrates is critical for determining the overall sustainability of the anaerobic degradation process. For instance, although biogas is considered environmentally friendly, the production of biogas using energy crops is associated with intensive land use change [2], emissions of greenhouse gases [3] and biodiversity loss [4]. These drawbacks are principally eradicated by the use of biomass residues remaining from agricultural or industrial production. As a consequence of the legislative changes, a major share of newly installed plants for biomethane production within the European Union use agricultural residues (manure and plant residues) [5]. Nevertheless, further research is needed to enable the effective anaerobic degradation through pre-treatment of such biomass residues, which are often composed of lignocellulosic biomass posing some recalcitrance towards anaerobic degradation.

Conventional pre-treatment methods such as acid and alkaline treatments face significant drawbacks, including high operational costs, corrosion of equipment, and environmental concerns due to the use of highly corrosive or acidifying chemicals or solvents [6]. While ionic liquids have been proposed as alternatives too, their non-biodegradability and the difficulty of removal from treated biomass pose additional challenges [6]. In contrast, deep eutectic solvents (DES) emerge as a promising alternative, offering efficient lignocellulosic fractionation with good lignin selectivity while employing less harmful, recyclable chemicals that retain their functionality over multiple cycles [7]. DES pose an option for valorising lignocellulosic biomass and producing value-added products [8]. They are a class of solvents composed of a hydrogen bond donor (HBD) and a hydrogen bond acceptor (HBA) substance. This composition allows the solvent to form a large number of hydrogen bonds, which explains why the melting point of the DES is substantially lower than the melting points of the individual substances [9]. Additionally, this property contributes to the excellent solvation capabilities of DES [10]. Quaternary ammonium salts such as choline chloride are frequently used as HBAs and are regularly combined with organic acids as HBDs [11]. DES are regarded as greener compared to conventional solvents because they are non-toxic and have a good biodegradability, recyclability and reusability [12]. Also they are seen as safter due to their low vapor pressure, thermal stability and non-flammable properties [13]. However, as this depends strongly on the composition of the DES mixture, this general categorization is not always justified [14] and should be challenged individually in each case.

Studies demonstrated that DES have the capability to dissolve lignin structures [15]. This is significant because lignin is considered a promising source of bio-aromatic components [16]. Thus, DES treatment opens the door to extract, e.g., phenolic compounds from biomass [17]. This approach carries a dual benefit: it facilitates the production of biogenic phenolic compounds and addresses the inherent recalcitrance towards anaerobic degradation of lignocellulosic biomass closely linked to the lignin content of such biomass streams. For the present study, choline chloride and formic acid were selected as components of the DES due to their lignin-selective solvation properties [18], effectively addressing lignin's role in recalcitrance to anaerobic degradation. This choice ensures that the glucan fraction is largely preserved, maintaining its integrity for further processing [19].

Against this background, in the present investigation, different residual lignocellulosic biomass streams from the cork and olive processing industry, which underwent a previous valorization step for phenol extraction by means of DES [8], were studied for a subsequent use as biogas substrate. In this way, the processing residues can be used for renewable energy production via biochemical conversion as part of an innovative integrated biorefinery concept. The novelty of this research lies in the selection of these very diverse substrates as well as in the respective pre-treatment method. The analysed biomasses are originating from the cultivation of olives (specifically: olive tree pruning), by-products from the cork stopper industry (specifically: cork dust, also referred to as cork powder), and residues from constructed wetlands (specifically: common reed) where wastewaters produced during the processing of cork bark and olives are treated. The substrates represent a wide spectrum of biomasses with very different properties. The aim is to investigate the impact of the DES pre-treatment on the composition of the solid residues of these diverse biomass streams. Ultimately, the overarching aim of the study is to assess the suitability of the solid waste streams remaining after the DES pre-treatment for biogas production. Therefore, specific emphasis is put on evaluating whether the DES-induced delignification process offers benefits to the anaerobic degradability and/or impacts the degradation kinetics.

2. Materials and methods

2.1. Procedure

The procedure of biomass processing and the scope of the investigation, as well as the respective experimental and analytical procedures are presented in Fig. 1. The residual biomass underwent DES treatment as specified, thereafter, the solid residues of the pre-treatment process were analysed for their biomass composition, as well as their anaerobic degradability. The focus here was exclusively on these solid residues, while the liquid phase, which is the main product provided during the treatment with DES, was not considered here (for more insights please refer to Ref. [8]).

2.2. Substrates

The cork dust was obtained from an industrial cork producer in Ponte de Sôr, Portugal. The olive tree pruning was collected from an olive orchard in Ayvalık, Turkey, and the common reed was harvested from Lake Mogan in Ankara, Turkey. Cork dust and olive tree pruning had a powdery structure, common reed was milled to a particle size <1 mm using a cutting mill (MF10, IKA, Germany).

2.3. DES pre-treatment

2.3.1. Preparation of DES

The choice for the composition of DES was based on the lignin-selective solvation properties of choline chloride and formic acid [18], which effectively reduce lignin's recalcitrance while preserving the glucan fraction for further processing [19]. The DES was prepared by mixing choline chloride (ChCl; 98 %; Sigma-Aldrich, USA) and formic acid (FA; 98–100 %; Supelco/Sigma-Aldrich, USA) at a molar ratio of 1:2. The substances were heated in a shaker incubator at 30 °C and 180 min^{-1} for approximately 2 h to form a transparent liquid [9]. The solvent was then heated overnight at 80 °C [19] and cooled to room temperature thereafter.

2.3.2. DES pre-treatment

10 g of biomass was mixed with the solvent at a 1:10 (g mL^{-1}) solid to solvent ratio (SSR) and then treated in an autoclave (NUVE, Turkey) at 90, 110, and 130 °C for 20, 40, and 60 min each. After this, the

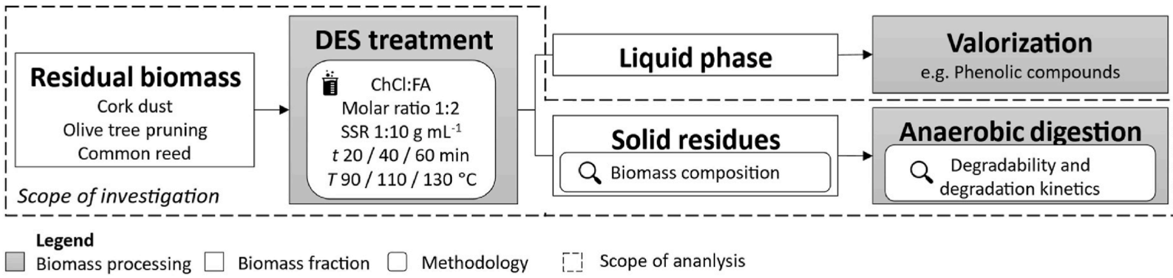

Fig. 1. Study design (ChCl choline chloride, FA formic acid, SSR solid to solvent ratio, *t* time, *T* temperature).

samples were cooled down in an ice bath. A subsequent liquid-solid separation was done using a vacuum filtration unit and coarse filter papers. While the liquid fraction underwent further investigations for valorization [8], the solid fraction was rinsed with 250 mL de-ionized water and subsequently dried for 2 d at 45 °C.

2.3.3. Solid recovery

The solid recovery *SR* was calculated from the mass of the dry sample before treatment m_0 and its mass after treatment m_t according to equation (1).

$$SR = (m_t \,/\, m_0)\ 100\ \% \tag{1}$$

2.4. Biomass composition

2.4.1. Dry mass and volatile solids content

The dry mass (*DM*) and volatile solids (*VS*) content of the biomass were determined gravimetrically according to Refs. [20,21], respectively. Drying took place overnight in an oven (U80, Memmert, Germany) at 105 °C. The analysis was performed in triplicate. The dry mass content *DM* was calculated from the fresh mass of the sample before drying m_f and the mass of the dry sample m_d as shown in equation (2).

$$DM = \left(m_d \,/\, m_f\right)\ 100\ \% \tag{2}$$

The samples were then incinerated in a muffle furnace (M104, Thermo Scientific Heraeus, USA) to determine volatile solids content *VS* which was calculated from the mass of the ashed sample m_a and the dry mass of the sample m_d according to equation (3).

$$VS = (1 - (m_a \,/\, m_d))100\ \% \tag{3}$$

2.4.2. Carbohydrate and lignin content

The macromolecular composition, i.e., the structural carbohydrate and lignin content of the dry samples, was determined according to the respective NREL laboratory analytical procedure [22]. This procedure uses a two-step acid hydrolysis to fractionate the biomass. The acid-insoluble solids are corrected for ash and reported as lignin. The solubilized sugar (i.e., glucose, xylose, arabinose, galactose, and mannose) concentrations were measured using a Dionex ICS-6000 system (Themo Scientific, USA) equipped with a pulsed amperometric detection unit (HPAEC-PAD). CarboPac PA200 column (thermos Scientific, USA) and a respective guard column were used for separation. For sample elution, an isocratic eluent of 2 mM sodium hydroxide with a flow rate of 0.35 mL min^{-1} at 30 °C was applied for 35 min. Quantification was done using a dilution series of sugar standards (glucose (≥99.5 %), xylose (≥99.0 %), mannose (≥99.0 %), galactose (≥99.0 %), arabinose (≥99.0 %); Sigma-Aldrich, USA).

2.4.3. Fourier-transformation infrared spectrophotometry

Fourier-transformation infrared spectrophotometry (FTIR) spectra of the dry biomass samples were recorded with a Vertex 70 spectrometer (Bruker Optik, Germany). The Spectrometer was equipped with a single bounce diamond ATR insert (MIRacle, Pike Technologies, USA) and a liquid-cooled MCT detector. Before the measurement, the instrument was purged with dry, carbon-free air. The FTIR spectra were recorded in a range from 4000 to 600 cm^{-1} with 200 scans per spectrum. The software OPUS (OPUS 7.0, Bruker) was used for recording and data processing including baseline correction.

To evaluate the effect of the treatment on the cellulose crystallinity, the crystallinity ratio *CR* was calculated according to equation (4) [23].

$$CR = a_{1,372} / a_{2,900} \tag{4}$$

a is the absorbance at the respective wavenumber. The peak at 1372 cm^{-1} (C-H bending) indicates changes in crystallinity of the biomass, and the 2900 cm^{-1} peak (C-H stretching in CH_2, peak maximum here: 2926 cm^{-1}) is usually rather unaffected by crystallinity changes. A higher *CR* indicates higher crystallinity in the cellulose structure [23].

To assess the effect of the treatment on the biomass composition, the cellulose to lignin ratio *CL* was calculated according to equation (5) [24].

$$CL = \left(a_{1,425} + a_{1,160}\right) / a_{1,515} \tag{5}$$

a is the absorbance at the respective wavenumber. The peak at 1425 cm^{-1} is related to native cellulose (type I) [24]. Amorphous cellulose types I and II are reflected in the peak at 1160 cm^{-1} [25]. The 1515 cm^{-1} peak is caused by lignin aromatic ring skeletal stretching [26].

2.5. Anaerobic degradability

2.5.1. Biogas and methane potential

The biogas potential of the dry biomass is determined according to the VDI guideline 4630 [27]. The experiments were performed in three runs – one run for each biomass type, and each sample was measured in triplicate. The anaerobic digestion batch tests were carried out in 500 mL glass reactors, which were placed in a climate chamber equipped with a floor heating system to provide mesophilic conditions (i.e., 37 ± 1 °C). An even temperature distribution was ensured by a fan. These reactors were connected to eudiometer tubes filled with sodium chloride and citric acid solution to capture the produced biogas. The reactors were filled with 400 mL sewage sludge (wastewater treatment plant Seevetal, Germany) as inoculum, which was allowed to outgas for at least 7 d. Thereafter, 2 g_{VS} of biomass were added to every reactor, and the headspace was purged with N_2 gas. The experiments were run for 60 d. Meanwhile, the reactors were mixed on a daily basis using a magnetic stirrer. The produced biogas volume V was measured using the eudiometer tubes, and the volume of dry gas at standard conditions $V_{dry,N}$ was calculated using equation (6).

$$V_{dry,N} = V\ \frac{(p - p_w)\ T_N}{p_N\ T} \tag{6}$$

p is the ambient pressure, p_w is the water vapor pressure calculated from the Magnus formula [28], and p_N is the normal pressure. T_N is the normal temperature ($T_N = 273$ K) and T is the ambient temperature. The biogas potential Y_{BG} was subsequently derived by dividing the volume $V_{dry,N}$ by the organic mass m fed to the reactors according to equation

(7).

$$Y_{BG} = V_{dry,N}/m \tag{7}$$

The composition of the biogas was measured using a portable gas analyzer (Biogas 5000, Geotech, UK) equipped with infrared sensors for CH_4 and CO_2 measurements, as well as a chemical sensor for measuring O_2. N_2 is measured as balance. The measurement error of the device is ±0.5 %. It was assumed that the dry gas in normal state consists of CO_2 and CH_4 only.

2.5.2. Kinetic parameters of anaerobic degradation

Five common and well-established kinetic models were applied to determine the kinetic parameters of the anaerobic digestion: the Modified Gompertz Model (equation (8)), the Logistic Function Model (equation (9)), the Transference Function Model (equation (10)), the First Order Kinetics (equation (11)) [29] and the Cone Model (equation (12)) [30].

$$P = P_0\, exp\left[-\,exp\left(\frac{R_m\, e}{P_o}(t-\lambda)+1\right)\right] \tag{8}$$

$$P = \frac{P_0}{1+exp\left(\frac{4R_m\,(\lambda-t)}{P_0}+2\right)} \tag{9}$$

$$P = P_0\left[1-exp\left(\frac{-R_m\,(t-\lambda)}{P_0}\right)\right] \tag{10}$$

$$P = P_0\,(1-\exp(-k_h\, t)) \tag{11}$$

$$P = \frac{P_0}{1+(k_h\, t)^{-s}} \tag{12}$$

P is the cumulative biogas production at time t, P_0 the maximum biogas yield, R_m the maximum biogas production rate, t the time, λ the lag phase, e the Euler's number, k_h the rate constant, and s a shape factor. The model fitting was performed using a nonlinear least squares method on the mean experimental biogas production. This approach minimizes the sum of the squared differences between the observed data and the values predicted by the model, iteratively adjusting the model parameters.

2.6. Statistical analysis

The Tukey post hoc test was used to assess the statistical difference between values at a level of significance of $\alpha = 0.05$.

3. Results and discussion

The results and discussion section is sub-structured into the two major subjects, namely the biomass composition (section 3.1) and the biogas and methane production (section 3.2), both being evaluated in the light of the treatment in the following.

3.1. Biomass composition

3.1.1. Cork dust

The composition of untreated cork dust was dominated by lignin (Fig. 2A). The untreated cork dust had a lignin content of 54.1 ± 1 %. The glucose and the xylose content were both below 10 % (Fig. 2A). The displayed lignin content was most likely composed of a major share of suberin as well. The respective FTIR spectrum (Fig. 3A) supports this assumption. This conclusion is justified due to the presence of major suberin peaks, namely peak a, b, c, j, and p in Fig. 3A. The attribution of the structures associated with the peaks of all FTIR spectra is shown in Tables 1 and 2. The lignin content for cork biomass reported in literature is usually lower compared to the results outlined above, ranging around 22 [31] to 25 % [32]. The reason for this deviation might be that the measurement method used here was not able to distinguish between lignin and suberin, but cork may contain more than 40 % of suberin [32] and for cork powder a suberin content of 11 % is reported [33]. Cellulose and hemicellulose contents are in accordance with literature [34].

As a consequence of the treatment, the glucose content increased with treatment temperature from 9.0 ± 0.2 % (untreated) to 17.2 ± 0.0 % (130 °C, 60 min). The xylose content of the treated samples ranged from 2.6 ± 0.6 % (90 °C, 60 min) to 6.3 ± 0.1 % (130 °C, 60 min). Thus, it was lower compared to the original sample (8.8 ± 0.1 %), showing a negative correlation with treatment temperature. The lignin content was slightly higher in the treated samples compared to the untreated sample, but the increase was not as clear as in the case of glucose.

Many of the FTIR peaks increased with treatment severity. Notably, both the suberin (a, b, c, d, e, i, j, p) and lignin peaks (d, e, f, g, i), as well as the cellulose peaks (mostly k and n in Fig. 3A and Table 2) increased with treatment severity. The relative concentration of the glucan fraction compared to lignin is also reflected in the cellulose to lignin ratio (*CL*) derived from the FTIR spectra of cork dust (Fig. 4). The *CL* ratio of all pre-treated samples was higher than the *CL* ratio of the untreated sample. Despite one outlier (110 °C, 40 min), this index increased with treatment temperature and duration. The untreated samples showed a *CL* ratio of 0.56, which increased to a maximum of 1.12 after a treatment at 130 °C for 60 min. The crystallinity ratio (*CR*) reflects the proportion of crystalline vs. amorphous cellulose in the sample (Fig. 4). The data indicates that the cellulose crystallinity was highest in the untreated sample (*CR* of 0.21). The samples treated for 60 min had the lowest

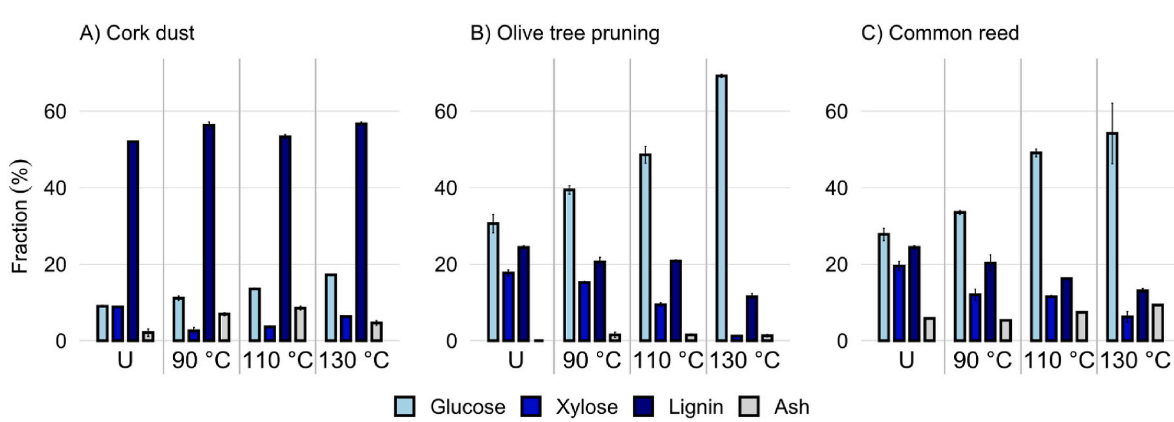

Fig. 2. Biomass composition of untreated (U) and treated A) cork dust, B) olive tree pruning and D) common reed of samples. Duration of DES treatment was 60 min, treatment temperature as indicated.

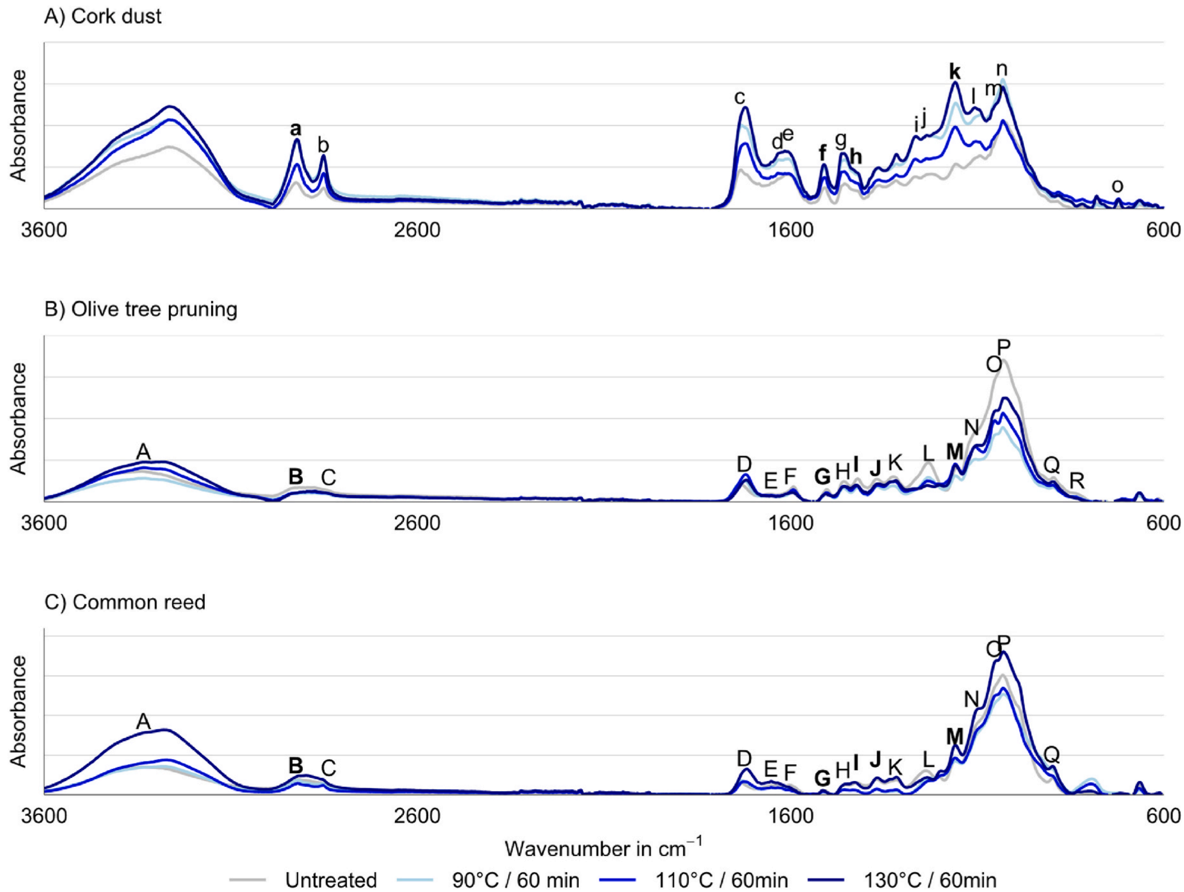

Fig. 3. FTIR spectra of untreated and treated A) cork dust, B) olive tree pruning and C) common reed biomass samples. Major peaks are marked with small (cork dust) and capital letters (olive tree pruning and common reed). Labels are resolved in Tables 1 and 2. Bold letters: peaks used for calculation of the *CR* and *CL* ratios.

crystallinity, with a *CR* of 0.12 (90 °C), 0.12 (110 °C), and 0.13 (130 °C), respectively.

3.1.2. Olive tree pruning

The dominant component within the untreated olive tree pruning was glucose with a fraction of 30.6 ± 2.4 %, followed by xylose and lignin, each around 20 %. These results are in agreement with literature [35].

After the DES treatment, the glucose content of olive tree pruning increased from 30.6 ± 2.4 % (untreated) to 69.2 ± 0.4 % (130 °C, 60 min) (Fig. 2B). Opposingly, the xylose and lignin content decreased with treatment temperature; i.e., the xylose content decreased from 17.7 ± 0.8 % (untreated) to 1.2 ± 0.1 % (130 °C, 60 min) and the lignin content decreased from 24.4 ± 0.4 % (untreated) to 11.5 ± 0.8 % (130 °C, 60 min).

In the FTIR spectrum of the olive tree pruning samples, lignin deformation is visible as some major lignin peaks decreased in height after the DES treatment compared to the untreated sample. For example, this is true for the peaks F, I, L, N, and P in Fig. 3B; some of these peaks are also related to the presence of cellulose (N and P in Fig. 3B). Another characteristic cellulose peak is peak O. Peak N and O appear to be lower but more pronounced in the treated samples (Fig. 3B). The increase in glucose corresponds to an increase in the cellulose to lignin ratio (*CL*) (Fig. 3B). This *CL* ratio increased considerably with treatment temperature and duration. The *CL* ratio of the untreated olive tree pruning was 0.73, and the highest measured *CL* ratio was 5.40 for the second harshest treatment (130 °C, 40 min). The cellulose crystallinity *CR* showed a decreasing trend with treatment severity, i.e., it decreased from 1.14 (90 °C, 20 min) to 0.56 (130 °C, 60 min).

3.1.3. Common reed

The major constituent of the untreated common reed was glucose with a share of 27.8 ± 1.6 %, while xylose and lignin each accounted for around 20 %. The cellulose content of common reed was comparably low (often above 40 %), while the hemicellulose matches literature (mid 20 % range), and the lignin content was comparably higher (often below 15 %) [36,37]. This atypical composition could be related to the fact that the plants were harvested at a relatively young age and from different locations.

The glucose content of common reed increased from 27.8 ± 1.6 % (untreated) to 54.2 ± 7.9 % (130 °C, 60 min). The xylose content decreased from 19.5 ± 1.2 % (untreated) to 6.2 ± 1.4 % (130 °C, 60 min), and the lignin content decreased from 24.4 ± 0.4 % (untreated) to 13.0 ± 0.6 % (130 °C, 60 min).

The FTIR spectra of the untreated and the harshest treated common reed samples are similar to each other in major regions of the spectra (e.g., the peaks G to K in Fig. 3C) related to different lignin and cellulose structures. At the same time, the spectral lines of the mild and medium harsh pre-treated samples follow a similar shape. Major differences can be observed, for e.g., the prominent peak A (Fig. 3C), which is caused by lignin structures and which was much higher after the harshest pre-treatment compared to all the other samples. Also, the most prominent cellulose peak P (Fig. 3C) was clearly higher after the harshest pre-treatment, and the cellulose peak N visible as a shoulder was more pronounced in that sample – analogously to the observations made for olive tree pruning. Similar to cork dust and olive tree pruning, the increase in glucose compared to lignin was also reflected in an increase in the FTIR-based cellulose to lignin ratio (*CL*). The *CL* ratio of the untreated sample was considerably lower (0.50) than the *CL* ratio of all treated samples. Even though not following a strict order, the *CL* ratio

Table 1
Assignments of peaks in the FTIR spectrum of cork dust with the label in Fig. 3A, the approximate band maximum of the peak (cm^{-1}), the associated vibration and related structure, and sources used for the assignment of the peaks.

Label Fig. 3	approximate band maximum (cm^{-1})	Vibration	Assignment/ related structure[a]	Source
a	2926	C-H stretch	Suberin, aliphatic	[52]
b	2852	C-H stretch	Suberin, aliphatic	[52]
c	1737	C=O stretch	Suberin, ester groups,	[52]
d	1635	C=C stretch	Suberin, aliphatic	[53]
e	1607	C=C stretch	Lignin, aromatic; extractives	[53]
f	1515	C=C stretch	Lignin, aromatic, G units	[53]
g	1465	CH_2 deformation stretch	Lignin	[54]
h	1425	C-H in-plane bending, CH_2 symmetric bending	Native cellulose type I	[24]
i	1263	C-O stretch	Suberin, hemicellulose, cellulose, lignin	[53]
J	1242	C-O-C stretch	Suberin	[55]
k	1160	C-O-C stretch	Cellulose I and II; hemicellulose	[24]
l	1110	C-OH deformation	cellulose, hemicellulose	[24]
m	1055	C-O stretch	Cellulose, hemicellulose	[24]
n	1034	C-H, C-O deformation	Cellulose, hemicellulose	[53]
o	724	$CH=CHR_2$	Aliphatic suberin	[55]

[a] assignment most often not limited to one biopolymer but rather associated with multiple biopolymers [53]. The assignment is based on the most prominent structure in the cited references, e.g. according to Ref. [56].

seemed to increase with treatment severity. The maximum *CL* ratio of 6.00 was determined for a treatment at 130 °C, 20 min. The cellulose crystallinity (*CR*) of the common reed samples showed an opposing trend compared to olive tree pruning and cork dust. Although the untreated sample had the highest *CR* (0.50), indicating a higher crystallinity of this sample compared to most pre-treated samples, the remaining data indicates an increasing crystallinity with treatment severity. This rather contradicts the expectations and the data obtained for cork dust and olive tree pruning.

3.1.4. *Comparative discussion*

The compositional and structural analysis of the samples suggests that the DES treatment resulted in lignin deformation and delignification. This effect was explicitly apparent for olive tree pruning and common reed, as the respective lignin content decreased with treatment severity. Even though this was not the case for cork dust, due to the loss of biomass as a consequence of the treatment (section 3.1.1.) and because an increase in cellulose was detected, this biomass also underwent delignification. The removal of the xylan (xylose) fraction observed for all biomasses indicates a dissolution of hemicellulose components into the liquid fraction. Meanwhile, the cellulose was relatively enriched in the biomass streams due to the removal of lignin and hemicellulose. This conclusion was supported by the increase or, in some cases more pronounced, cellulose peaks in the FTIR spectra, as well as by the increased *CL* ratio of the treated samples.

Lynam et al. [24] observed this increase in the *CL* ratio of DES-treated loblolly pine wood samples (ChCl:FA 1:2 M ratio, SSR 1:10, *T* 155 °C, *t* 120 min). While the solid remaining contained higher amounts of cellulose after treatment, a lignin-rich precipitate could be obtained from the liquid fraction thereafter [24]. Tan et al. [38] reviewed the effect of different DES treatments on biomass composition.

Table 2
Assignments of peaks in the FTIR spectrum of olive tree pruning (Fig. 3B) and common reed (Fig. 3C) with the respective label in the Figure, the approximate band maximum of the peak (cm^{-1}), the associated vibration and related structure, and sources used for the assignment of the peaks. G: guaiacyl units of lignin, S: syringyl units of lignin, H: *p*-hydroxyphenylpropane unit of lignin.

Label Fig. 3	approximate band maximum (cm^{-1})	Vibration	Assignment/ related structure	Source
A	3334	O-H stretch	Aromatic & aliphatic lignin	[57]
B	2926	C-H stretch	CH_2 group	[26]
C	2838	C-H stretch	CH_3 group	[57]
D	1724	C=O stretch	Nonconjugated ketones & esters	[57]
E	1653	C=O stretch	Lignin, conjugated ketones	[57]
F	1601	aromatic skeleton stretch, C=O stretch	Lignin	[58]
G	1515	aromatic skeleton stretch	Lignin, aromatic ring	[24]
H	1460	asymmetric C-H bending	$-CH_2-$ and CH_3	[58]
I	1425	C-H in-plane bending, CH_2 symmetric bending	native cellulose type I	[24]
J	1372	symmetric C-H bending	CH_3, aliphatic compounds	[23]
K	1320	aromatic ring breathing	Lignin, G and S units	[58]
L	1230	C-C, C-O, C=O stretch		[26]
M	1160	C-O-C stretch	Cellulose I and II and hemicellulose	[26]
N	1115	C-H in-plane bending, C-OH skeletal vibrations	Lignin, S units, Cellulose	[58]
O	1055	C-O, C-O-C stretch	Cellulose, hemicellulose	[26]
P	1029	C-O stretch	Cellulose	[58]
Q	901	C-H deformation	Cellulose, saccharides	[26]
R	833	C-H out-of-plane bending	Lignin, S and H units	[58]

The glucan fraction – i.e., the glucose/cellulose fraction – was commonly substantially less affected by DES treatment than the xylan and lignin fraction [38]. Moreover, acid-based DES, like the choline chloride:formic acid mixture used in this study, are reported to be more effective in removing lignin and xylan than other DES mixtures [38]. For example, Yu et al. [39] reported a retention of 98 % of the glucan fraction in ChCl:FA pre-treated herbal residues (ChCl:FA 1:2 M ratio, SSR 1:10, *T* 120 °C, *t* 8 h) while more than 40 % of the lignin was solubilized. The same study revealed that the lignin solubilization was strongly related to the presence of choline chloride, while acid treatment alone did not lead to a substantial lignin removal [39]. Additionally, the acidic component of the DES mixture is contributing substantially to the removal of the xylan fraction [40]. Lynam et al. [24] tested glycerol as a blank treatment at the same treatment conditions (temperature and time) as the DES. They observed little or no effect in terms of lignin deformation or removal, suggesting that the reported effects can be attributed to the use of DES [24].

Lignin is composed of phenolic compounds such as p-hydroxyphenyl (H), guaiacyl (G), and syringyl (S), which are mainly connected by aryl ether (C–O) and carbon-carbon (C–C) bonds [41]. In the process of lignin removal using DES, the key mechanism involves breaking the aryl ether (C–O) and carbon-carbon (C–C) linkages in lignin [41]. Additionally, DES helps to disrupt the covalent bonds between lignin and hemicellulose and the hydrogen bonds between lignin and cellulose. Other reactions, such as hydroxylation and demethoxylation, may also occur

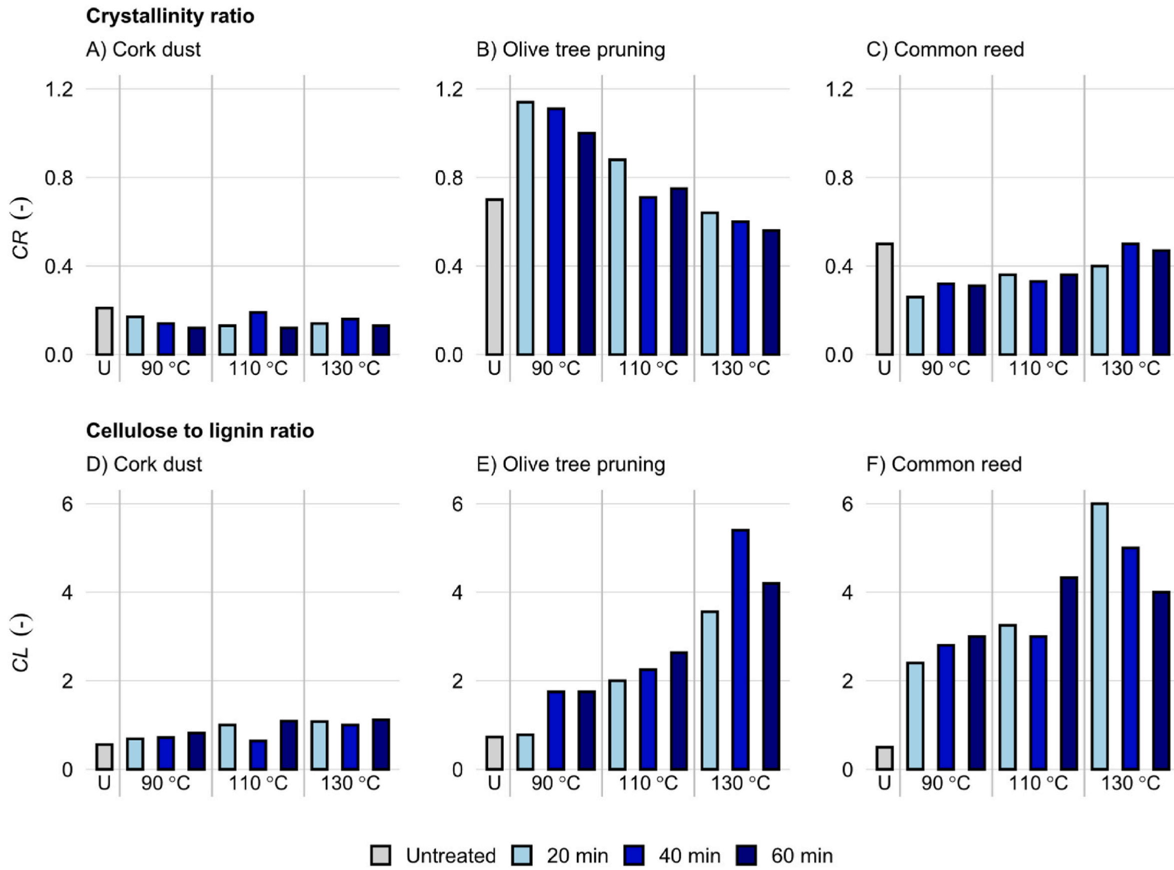

Fig. 4. top: *CR* ratio of A) cork dust and B) olive tree pruning and C) common reed; bottom: *CL* ratio of D) cork dust and E) olive tree pruning and F) common reed of untreated (U) and DES treated samples.

during this process. C–C bonds are more resistant to cleavage compared to C–O bonds due to their higher bond dissociation energies [41].

Loow et al. [42] pointed out that the delignification mechanism of biomass using chlorine-based deep eutectic solvents (DES) is primarily driven by the formation of hydrogen bonds between the halogen anions in the DES and lignin. Halogen anions, such as Cl^-, can form hydrogen bonds with the hydroxyl (−OH) groups in lignin, resulting in lignin dissolution and the extraction of aromatic compounds. Consequently, the efficiency of delignification is closely linked to the ability of the electronegative halogen anion in the DES to form hydrogen bonds with lignin [43]. In addition, the removal of plant cell components, such as xylan and lignin, during DES pre-treatment may be attributed to protons (H^+) dissociated from formic acid, the hydrogen bond donor (HBD). These protons could catalyze the cleavage of ether or ester bonds between lignin and hemicellulose [44].

The cellulose crystallinity (*CR*) did not show such clear results as the compositional analysis. Excluding the original sample, the *CR* of cork dust and olive tree pruning decreased with treatment severity, the treated common reed also had a lower crystallinity, but the *CR* of common reed increased with treatment severity. In fact, a reduction in cellulose crystallinity and polymerization is regarded as favourable for subsequent anaerobic digestion, as highly crystalline structures hinder enzyme accessibility and many chemical forms of pre-treatment are aimed specifically at this [45]. Even though the present DES treatment resulted tendentially in a decreased crystallinity, this trend is not consistent across the biomass types and treatment conditions. This ambiguity is also evident when looking into literature. For example, cellulose crystallinity of poplar wood was reported to decrease as a consequence of DES treatment (choline hydroxide:urea, 1:2 M ratio, SSR not given, *T* 60 °C, *t* 2–10 min, [46]). However, most often DES treatments are associated with an increase in crystallinity. This effect was reported for DES treated oil palm fronds (ChCl: urea, 1:2 M ratio, SSR 1:10 (w/v), *T* 120 °C, *t* 240 min [47] rape straw (ChCl:OA (oxalic acid) varied molar ratios, SSR 1:10 (w/w), *T* 90–140 °C, *t* 60 min [48]) and walnut shells (ChCl: p-toluene-sulfonic acid: ethylene glycol, molar ratio 1:1:2, SSR 1:10 (w/w), *T* 90 °C, *t* 90–180 min [49]). The increased crystallinity can be attributed to an exposure of crystalline cellulose due to lignin disintegration [49], as well as the removal hemicellulose [50] and amorphous cellulose [51].

3.2. Biogas and methane production

3.2.1. Cork dust

The untreated cork dust had a low biogas potential. The biogas and biomethane potential of untreated cork dust was only 51 ± 13 and 35 ± 9 $mL_N\ g_{VS}^{-1}$ (Fig. 5A and D), respectively. While investigations on the use of cork boiling wastewater for biogas production were reported before [59], cork dust has not yet been discussed in literature as a substrate for biogas production. Nevertheless, the biogas production can be regarded as extremely low compared to other substrates like corn stover, rice, or wheat straw [60]. Consequently, cork dust is not a preferred substrate for biogas production.

The DES treatment did not significantly impact the biogas potential at treatment temperatures of 90 and 110 °C (also referred to as “mild” treatment conditions hereafter), as illustrated in Fig. 5A. Even though the biogas potential after the treatment at 130 °C for 20 min was higher than the biogas potential of the original sample, the effect was only significant for the treatment at 130 °C for 40 and 60 min. The sample with the longest treatment time had a biogas potential of 115 ± 4 $mL_N\ g_{VS}^{-1}$. This represents an increase of +125 % or 63 $mL_N\ g_{VS}^{-1}$ compared to the untreated sample. Percentage-wise, this is the strongest increase in the biogas potential observed among all three considered biomass types.

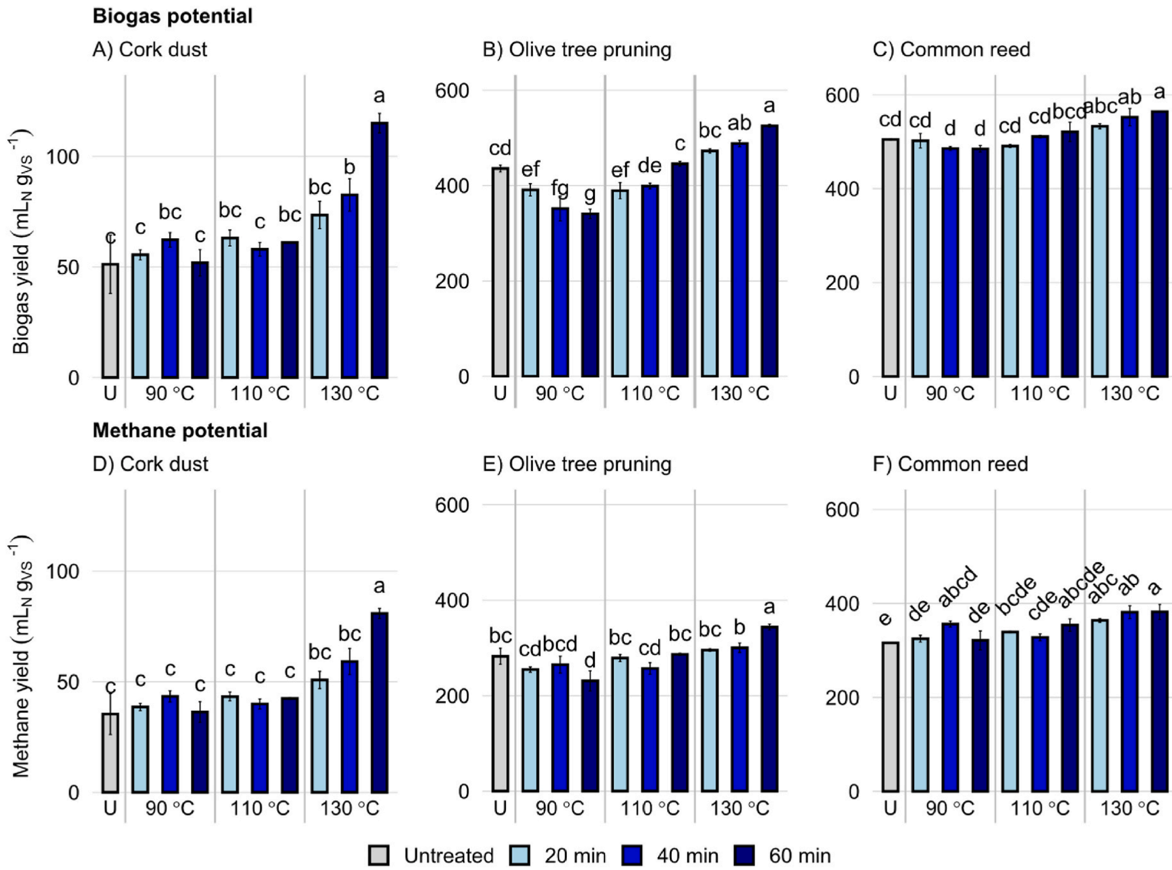

Fig. 5. Experimental biogas potential of untreated (U) and treated A) cork dust, B) olive tree pruning and C) common reed and methane potential of D) cork dust, E) olive tree pruning and F) common reed. The compact letter display (lower case letters) indicates significant differences between samples ($p < 0.5$). Notice that the axis scale of cork dust is substantially smaller than the ones of olive tree pruning and common reed.

Evaluating the treatment effect on the methane potential, a significant increase was only measured for the sample treated at 130 °C for 60 min. This sample had a methane potential of 81 ± 2 mL$_N$ g_{VS}^{-1} which is 128 % higher compared to the methane potential of the original sample (35 ± 9 mL$_N$ g_{VS}^{-1}, Fig. 5D).

The solid recovery, i.e., the fraction of biomass recovered after the treatment and subsequently used for the biogas testing, is depicted in Fig. 6A–C. As shown, the solid recovery decreased with treatment time and temperature and was lowest after a treatment at 130 °C and 60 min for all biomasses. The loss of biomass was substantial. For cork dust, the lowest solid recovery is determined to be 76 %. This means a loss of 24 % of substrate for biogas production. It should be noted that this is the recovery of the dry matter (including the inorganic fraction) before and after treatment, not only the organic matter. Nevertheless, an approximate comparison of the biogas obtained per organic mass with and without biomass loss can be made. If the loss of 24 % was subtracted from the gain in biogas of 125 %, the amount of biogas gained would be significantly reduced. As an approximation, the biogas yield would not have increased from 52 ml$_N$ g_{VS}^{-1} (original sample) to 115 ml$_N$ g_{VS}^{-1} (130 °C, 60 min) as a consequence of the treatment, but only to 87 mL$_N$ g_{VS}^{-1}.

3.2.2. *Olive tree pruning*

The untreated olive tree pruning had a biogas potential of 436 ± 7 mL$_N$ g_{VS}^{-1} (biomethane potential: 283 ± 17 mL$_N$ g_{VS}^{-1}, Fig. 5B and E). For

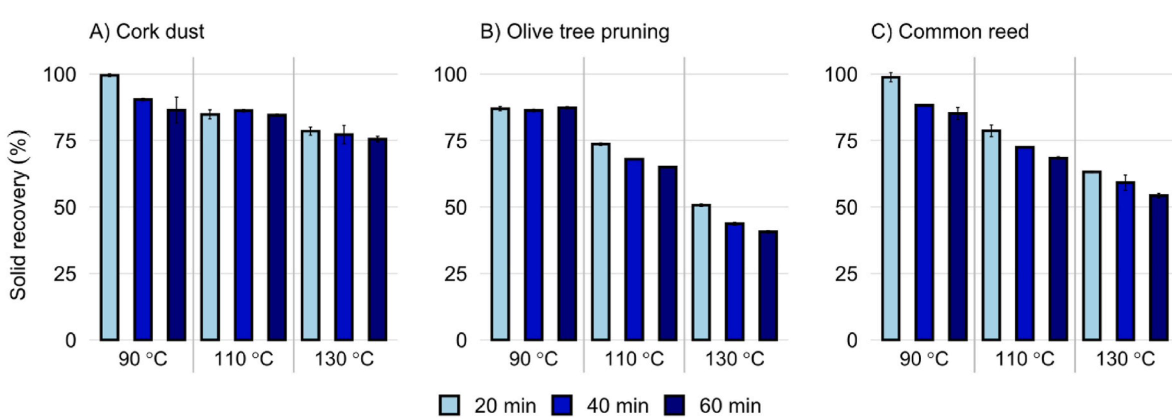

Fig. 6. Solid recovery of A) cork dust, B) olive tree pruning and C) common reed after DES treatment.

olive tree pruning only, scarce information on the anaerobic digestibility is available. For example, Nitsos et al. [61] measured a biomethane potential of 57 mL g_{VS}^{-1} for olive tree pruning (particle size <1 mm, thermophilic conditions) [61]. This is substantially lower compared to the biomethane potential of 283 ± 17 mL_N g_{VS}^{-1} determined here. Most likely, the particle size plays a decisive role, as supported by Bianchini et al. [62], who found variations in biomethane potential based on particle size [62]. Although the olive tree pruning analysed in this study had a powdery structure, the biogas potential was still remarkably high.

The biogas potential of the mildly treated olive tree pruning samples decreased significantly compared to the original sample (Fig. 5B). For instance, the olive tree pruning sample treated at 90 °C for 60 min had a biogas potential of 341 ± 10 mL_N g_{VS}^{-1}, which is 22 % lower than the biogas potential of the untreated sample (436 ± 7 mL_N g_{VS}^{-1}). Analogously to cork dust, after a treatment at 130 °C for 60 min, there was a significant increase in biogas potential. With a biogas potential of 525 ± 3 mL_N g_{VS}^{-1} the yield was 21 % or 90 mL_N g_{VS}^{-1} higher compared to the original sample – the most substantial increase in absolute numbers measured here. The methane potential of the sample treated at 130 °C and 60 min was 344 ± 6 mL_N g_{VS}^{-1}, being 22 % higher than the original sample (283 ± 17 mL_N g_{VS}^{-1}, Fig. 5E).

The loss of biomass reflected by the low solid recovery was particularly strong for the olive tree pruning samples. While a maximum increase of 21 % (130 °C, 60 min) was achieved, the solid recovery for this sample was only 41 %. This means that the treatment resulted in an absolute loss of biogas yield. A biogas production of 436 mL_N g_{VS}^{-1} (original sample) would then be offset by a biogas production of only 214 ml_N g_{VS}^{-1} (130 °C, 60 min).

3.2.3. Common reed

The untreated common reed had a biogas potential of 505 ± 1 ml_N g_{VS}^{-1} (biomethane potential: 316 ± 1 mL_N g_{VS}^{-1}, Fig. 5C and F). This is a remarkably high biomethane potential when compared with literature (e.g., 173 mL g_{VS}^{-1} (particle size <2 mm) [63] or 77 mL_N g_{VS}^{-1} (particle size <3 mm) [37]). This difference may be attributed to the small particle size (<1 mm) and the young age at harvest being atypical for common reed. For instance, Pizarro-Loaiza et al. [71] reported that harvesting age had an impact in the performance of anaerobic digestion of king grass [64]. Overall, olive tree pruning and common reed showed biogas and biomethane potentials that are competitive with more common agricultural residues suggested for biogas production [60].

The DES treatment did not affect the biogas potential under mild conditions (Fig. 5C). Once more, a significant increase was observed for the treated samples at 130 °C for 40 and 60 min. The biogas potential increased from 505 ± 1 mL_N g_{VS}^{-1} (untreated) to 565 ± 1 mL_N g_{VS}^{-1} (130 °C, 60 min) by 12 % or 60 ± 1 mL_N g_{VS}^{-1}. The methane potential rose from 361 ± 1 mL_N g_{VS}^{-1} (untreated) to 382 ± 16 mL_N g_{VS}^{-1} (130 °C, 60 min), accounting for an increase by 7 % or 21 mL_N g_{VS}^{-1} (Fig. 5F).

Analogously to cork dust and olive tree pruning, the consideration of solid recovery diminishes the produced biogas from the original biomass. Considering the solid recovery of 54 %, the harshest pretreated sample had a biogas potential of 307 mL_N g_{VS}^{-1}.

3.2.4. Comparative discussion

DES pre-treatment resulted in increased biogas and biomethane production across all investigated biomass streams, even though the absolute and relative increase differed considerably. A notable increase in biogas potential was primarily observed under relatively harsh pretreatment conditions, since a statistically significant increase in biogas potential was only observed at a temperature of 130 °C. When comparing with literature, attention should be paid to the often dissimilar DES mixtures and treatment conditions employed. Still, parallels and differences to published results and findings can be drawn, as the mode of action of DES is generally similar.

Other studies have also documented an increased biomethane production under milder DES treatment conditions. Olugbemide et al. [65] reported an enhancement of biomethane production from corn stover's solid fraction by 48 % after DES treatment at 100 °C (ammonium thiocyanate and urea, molar ratios 1:1 and 1:2, SSR 1:2, *T* 100 °C, *t* 60 min [65]). Additionally, an investigation to optimize treatment conditions found that biomethane production is highest at temperatures as high as 160 °C. In a respective investigation, the biomethane yield of willow could be increased by 36 % as a result of DES treatment (ChCl:lactic acid, 1:10 M ratio, SSR 1:20, *T* 160 °C, *t* 15 min [11]). Sha et al. [66] could show that alkaline DES can also be effective when applied as pre-treatment for biomethane production from lignocellulosic biomass. They reported a comparably moderate increase in biomethane potential, but the treatment procedure differed significantly from the present study, making a comparison of the results inconclusive.

Considering the results of the compositional and structural analysis (section 3.1.) of the present investigation alongside the biogas tests, a coherent pattern emerges: both, the reduction of the lignin content (as observed for olive tree pruning and common reed) and the concurrent retention of the fermentable component cellulose in the solid biomass (evident across all investigated biomasses), were closely linked to the increase in biogas and biomethane potential. Other publications report similar effects of different DES mixtures in lignin removal and glucan retention. For example, Kang et al. [11] reported that lactic acid-based DES was effective in removing lignin, while retaining up to 94 % of the glucan fraction. They found that lactic acid-based DES was more effective than the acetic acid- and propionic acid-based DES. Similarly, Nawaz et al. [67] found lactic acid to provide a lignin removal of 89.5 % alongside a substantially increased biogas potential of the treated substrate *Atriplex crassifolia* (ChCl:lactic acid, 1:2 M ratio, SSR 1:15, *T* 120 °C, *t* 240 min), this was the highest removal among several carboxylic acids, polyols, glycols, amines and amides tested as HBD. In another investigation, using formic acid as the HBD proved to be the most effective for lignin removal during microwave-assisted DES treatment, compared to other carboxylic acids, including lactic acid [68].

Interestingly, the compositional changes caused by mild DES pretreatment did not enhance the biogas and methane potential of the biomasses. In fact, the biogas potential of olive tree pruning and common reed specifically decreased despite an increase in relative cellulose content at 110 °C. This outcome could be attributed to the removal of easily accessible hemicellulose and amorphous cellulose structures [51] under these conditions, without adequate lignin removal or significant changes in crystallinity. Even though changes in cellulose crystallinity are observed in the current investigation, they are inconsistent across the biomass types, and no clear trend could be identified with regard to its effect on the biogas and biomethane potential, suggesting that compositional changes were more significant for improving the biogas potential compared to structural changes. In fact, there are conflicting observations in literature regarding crystallinity alterations as discussed in section 3.1.4., suggesting that the effect on crystallinity strongly depends on biomass type and treatment conditions such as temperature and time. Still, physical alterations to lignocellulosic biomass have been linked to improved biomethane production [65] and both effects could support the microbial utilization of cellulose, e.g., for conversion to biogas. Firstly, an increased *CR* associated with the removal of non-fermentable components like lignin could improve the digestibility. Secondly, a reduction in crystallinity enables microorganisms to access and convert cellulose more efficiently [69].

As a consequence of the pre-treatment, a fraction of the biomass has been dissolved in the liquid phase. Actually, the pre-treatment is specifically intended to dissolve phenolics and other value-added products from the biomass [8]. While this is intentional to further valorize the dissolved fraction, it also affected the amount of biomass that is available for biogas production after the treatment. The considerable impact on the loss of solid material during DES treatment has previously been documented. Kang et al. [11] reported an increasing biomass loss with treatment temperatures ranging from 120 to 160 °C, with a solid recovery as low as 46.8 % (willow, ChCl:lactic acid, 1:10 M ratio, *T* 160 °C,

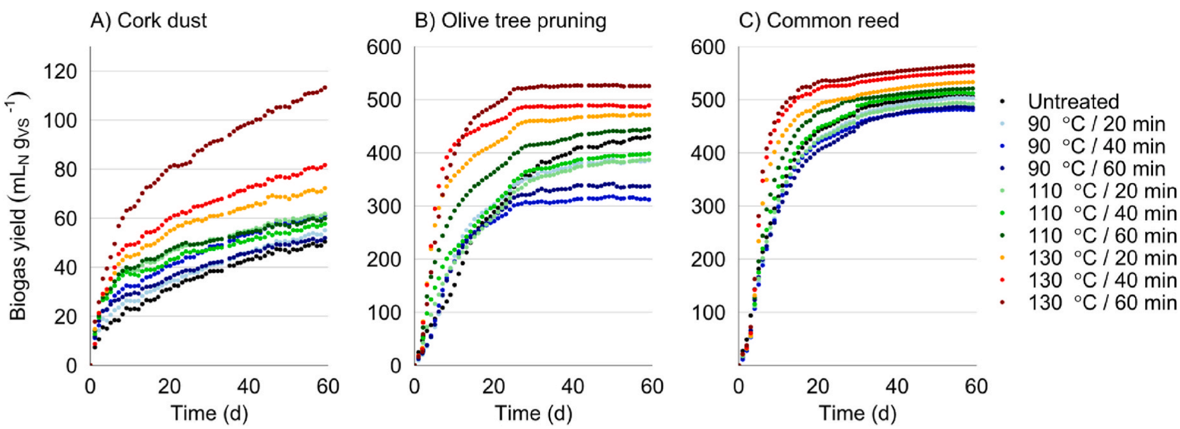

Fig. 7. Cumulative biogas formation over the course of the experiments of A) cork dust, B) olive tree pruning and C) common reed.

t 30 min [11]). The severe discrepancy between the increase of biogas on the one hand and the loss of biomass, which cancels out this effect completely, on the other hand, must lead to the conclusion that the DES treatment for an improved biogas yield alone is not recommended. Nevertheless, if the treated biomass is seen as a residue from a valorization process – in this case, valorization of the liquid fraction produced during pre-treatment – the use of the latter for biogas production can still hold significance within an overall and fully integrated biorefinery concept. In this light, mass loss would not necessarily be a disadvantage. The recovered liquid phase of such a biorefinery process contains components such as dissolved sugars, xylooligosaccharides [19] and phenolic compounds which are regarded as value-added products [44]. Under these conditions, treatment parameters would need to be optimized for the valorization step prior to biogas production, rather than solely for biogas production.

Table 3
Results of kinetic modelling of the anaerobic digestion of (DES treated) cork dust. Kinetic parameters of the Modified Gompertz Model, the Transference Model, the Logistic Function Model, the First Order Kinetics and the Cone Model. P_0: maximum biogas yield of substrate ($mL_N\ g_{VS}^{-1}$), R_m: maximum bigas production rate ($mL_N\ g_{VS}^{-1}\ d^{-1}$), λ: lag phase (d), k_h: rate constant (d^{-1}), s: shape factor (–), R^2: coefficient of determination (–), *RMSE*: root mean square error ($mL_N\ g_{VS}^{-1}$).

Cork dust											
T	°C	–	90	90	90	110	110	110	130	130	130
t	min	–	20	40	60	20	40	60	20	40	60
Modified Gompertz Model											
P_0	$mL_N\ g_{VS}^{-1}$	51.7	57.6	62.5	52.7	59.8	55.2	56.8	69.1	77.7	108.9
R_m	$mL_N\ g_{VS}^{-1}\ d^{-1}$	1.08	1.05	1.32	1.11	1.67	1.58	2.08	2.24	2.46	3.06
λ	d	−9.1	−12.7	−12	−14.1	−11.4	−11.5	−8.2	−8.4	−7.9	−8.5
R^2	–	0.977	0.965	0.955	0.941	0.908	0.892	0.906	0.934	0.928	0.944
RMSE	$mL_N\ g_{VS}^{-1}$	1.82	2.3	2.8	2.55	3.51	3.46	3.37	3.67	4.5	5.67
Transference Model											
P_0	$mL_N\ g_{VS}^{-1}$	55.9	62.3	65.2	54.4	60.4	55.6	57.2	70.1	78.9	111.5
R_m	$mL_N\ g_{VS}^{-1}\ d^{-1}$	1.89	1.87	2.55	2.24	3.68	3.54	4.61	4.77	5.17	6.2
λ	d	−4.2	−6.3	−5.5	−6.7	−4.7	−4.7	−3.1	−3.2	−2.7	−3.1
R^2	–	0.986	0.976	0.969	0.955	0.934	0.921	0.937	0.959	0.957	0.968
RMSE	$mL_N\ g_{VS}^{-1}$	1.41	1.94	2.37	2.27	3.06	3.05	2.85	2.98	3.6	4.41
Logistic Function Model											
P_0	$mL_N\ g_{VS}^{-1}$	49.8	55.4	61	51.7	59.4	54.9	56.5	68.6	77	107.5
R_m	$mL_N\ g_{VS}^{-1}\ d^{-1}$	1	0.95	1.16	0.96	1.36	1.27	1.68	1.86	2.04	2.59
λ	d	−10.5	−14.7	−14.8	−17.5	−15.4	−15.8	−11.5	−11.4	−10.8	−11.3
R^2	–	0.968	0.956	0.944	0.93	0.888	0.87	0.881	0.914	0.904	0.924
RMSE	$mL_N\ g_{VS}^{-1}$	2.11	2.55	3.1	2.74	3.81	3.73	3.72	4.12	5.07	6.5
First Order Kinetics											
P_0	$mL_N\ g_{VS}^{-1}$	50.4	53.2	58.6	48.6	56.6	52.2	55.1	67.1	75.7	105.8
k_h	d^{-1}	0.05	0.06	0.07	0.08	0.11	0.12	0.13	0.1	0.09	0.08
R^2	–	0.968	0.942	0.936	0.906	0.901	0.89	0.917	0.938	0.944	0.953
RMSE	$mL_N\ g_{VS}^{-1}$	2.39	3.38	3.86	3.79	4.26	4.07	3.64	4.07	4.44	5.87
Cone Model											
P_0	$mL_N\ g_{VS}^{-1}$	234.8	NA	316.9	329.3	107	94.3	79.7	104.7	115.7	187.5
k_h	d^{-1}	0	NA	0	0	0.03	0.04	0.09	0.06	0.06	0.03
s	–	0.5	NA	0.4	0.4	0.5	0.5	0.6	0.6	0.7	0.6
R^2	–	0.995	NA	0.993	0.989	0.986	0.98	0.988	0.993	0.989	0.994
RMSE	$mL_N\ g_{VS}^{-1}$	0.85	NA	1.15	1.14	1.43	1.55	1.23	1.23	1.83	1.99

Table 4
Results of kinetic modelling of the anaerobic digestion of (DES treated) olive tree pruning. Kinetic parameters of the Modified Gompertz Model, the Transference Model, the Logistic Function Model, the First Order Kinetics and the Cone Model. P_0: maximum biogas yield of substrate ($mL_N\ g_{VS}^{-1}$), R_m: maximum bigas production rate ($mL_N\ g_{VS}^{-1}\ d^{-1}$), λ: lag phase (d), k_h: rate constant (d^{-1}), s: shape factor (–), R^2: coefficient of determination (–), $RMSE$: root mean square error ($mL_N\ g_{VS}^{-1}$).

Olive tree pruning											
T	°C	–	90	90	90	110	110	110	130	130	130
T	min	–	20	40	60	20	40	60	20	40	60
Modified Gompertz Model											
P_0	$mL_N\ g_{VS}^{-1}$	428.2	377.5	310.8	335.1	383.5	393.1	429.9	457.2	478.9	520.6
R_m	$mL_N\ g_{VS}^{-1}\ d^{-1}$	15.23	20.52	21.13	19.62	15.03	16.48	24.13	39.73	63.99	48.07
λ	d	−0.2	1	1	0.9	−1.6	−2.2	−1.6	−0.4	0.9	0.8
R^2	–	0.997	0.99	0.994	0.994	0.989	0.98	0.969	0.96	0.982	0.991
$RMSE$	$mL_N\ g_{VS}^{-1}$	7.15	11.31	7.04	7.93	11.46	14.83	19.35	22.39	15.88	13.13
Transference Model											
P_0	$mL_N\ g_{VS}^{-1}$	462.1	393.2	319.2	345.9	398.4	403.6	437.6	464.3	486.5	529.5
R_m	$mL_N\ g_{VS}^{-1}\ d^{-1}$	23.27	31.39	32.52	30.64	26.01	30.02	44.47	67.35	89.44	74.4
λ	d	0.6	1.3	1.1	1.1	0.2	0	0.1	0.4	0.7	0.8
R^2	–	0.994	0.992	0.99	0.992	0.997	0.993	0.99	0.981	0.98	0.991
$RMSE$	$mL_N\ g_{VS}^{-1}$	10.16	10.54	8.96	9.19	5.5	8.76	11.22	15.88	17.13	13.63
Logistic Function Model											
P_0	$mL_N\ g_{VS}^{-1}$	418.1	372.6	307.9	331.7	378	388.8	426.5	453.9	476.4	517.4
R_m	$mL_N\ g_{VS}^{-1}\ d^{-1}$	14.76	19.79	20.49	18.71	13.88	14.87	21.65	37.57	64.87	46.61
λ	d	0.1	1.2	1.2	1	−2	−2.9	−2.2	−0.5	1.1	0.9
R^2	–	0.99	0.975	0.982	0.981	0.977	0.966	0.947	0.935	0.969	0.978
$RMSE$	$mL_N\ g_{VS}^{-1}$	12.6	17.49	11.68	13.24	16.17	19.03	24.58	27.57	20.37	20.18
First Order Kinetics											
P_0	$mL_N\ g_{VS}^{-1}$	468.1	400.3	322.7	350.6	399.8	403.3	438.2	466.2	488.9	533.1
k_h	d^{-1}	0.05	0.07	0.09	0.08	0.06	0.07	0.1	0.13	0.16	0.12
R^2	–	0.993	0.981	0.979	0.981	0.997	0.993	0.99	0.978	0.965	0.978
$RMSE$	$mL_N\ g_{VS}^{-1}$	10.85	14.91	12.41	12.89	5.67	8.76	11.28	16.77	20.88	19.55
Cone Model											
P_0	$mL_N\ g_{VS}^{-1}$	498.9	401.6	323.1	352.3	450	457.2	473.5	480.1	488.3	534.8
k_h	d^{-1}	0.06	0.1	0.12	0.11	0.08	0.09	0.14	0.19	0.22	0.17
s	–	1.5	1.9	2	2	1.3	1.2	1.3	1.6	2.2	2.1
R^2	–	0.995	0.998	0.998	0.998	0.996	0.993	0.995	0.989	0.995	0.999
$RMSE$	$mL_N\ g_{VS}^{-1}$	9.39	5.39	4.07	5.07	6.8	9.18	8.06	11.78	8.92	5.48

3.3. Kinetics of anaerobic degradation

Among all biomasses examined the DES treatment induced changes in the degradation kinetics. This effect is illustrated in Fig. 7 showing the cumulative biogas production. Notably, Fig. 7B (olive tree pruning) showcases this effect most clearly, with the treated samples, especially the sample treated at 130 °C for 60 min (red points), exhibiting a steep rise in biogas yield within the first 25 d. Subsequently, there was a low new formation of biogas for the respective sample, as illustrated by the near-horizontal line of red dots. Meanwhile, the original sample (black dots) had a less steep rise initially, and its biogas formation continued towards the end of the experiment.

The results of the kinetic modelling are shown in Tables 3–5. An exemplary visual representation in comparison to the measured data can be found in the supplementary material (Figures S.2 to S.31). All five models applied demonstrate a good fit across the various biomasses and pre-treatment conditions examined. The model with the best fit (R^2) and smallest $RMSE$ is the Cone Model for cork dust ($RMSE$ ranging from 0.85 to 1.99 $mL_N\ g_{VS}^{-1}$), olive tree pruning ($RMSE$ ranging from 4.07 to 11.78 $mL_N\ g_{VS}^{-1}$) and common reed ($RMSE$ ranging from 2.96 to 10.79 $mL_N\ g_{VS}^{-1}$). This indicates that the derived parameters are robust and makes them well-suited for applications such as modelling of continuous, large-scale processes [71]. The change in degradation kinetics is also reflected in the parameters of the kinetic models. For instance, the maximum biogas production rate R_m as determined by the Modified Gompertz Model, the Transference Model, and the Logistic Function Model mostly increases with treatment severity. Accordingly, the rate constant k_h as determined by the First Order Kinetics and the Cone Model increases with treatment severity (Table 3, Tables 4, and Table 5). The lag phase (λ) differs among the biomass types, for example, cork dust shows practically no lag phase with consistently negative λ values. The slightly longer lag phase of the degradation of common reed is reflected in positive λ values as well as in Fig. 7.

The DES treatment induced changes in degradation kinetics across all biomasses. Similar changes in the degradation kinetics were reported by Kang et al. [11] who observed a shift in the time needed to produce 80 % of the total methane yield from 22 d to as few as 10 d [11]. Analogously to the increase in biogas and methane potential, these changes were closely linked to the biomass composition. Similar findings have been reported, highlighting how the retention of the glucan fraction (cellulose) in the solid fraction and the removal of lignin due to DES treatment lead to enhanced enzymatic hydrolysis [15] and biomethane production [11]. DES pre-treated samples exhibited elevated concentrations of volatile fatty acids in the digestion slurry during the process of anaerobic degradation [11]. This confirms the assumption that a faster and more efficient hydrolysis is possible after lignin removal [11]. The kinetic behaviour of the DES-treated samples suggests that digestible components were not only available in higher quantities as the biogas production was increased, but the components were more easily and rapidly accessible to and degradable by microorganisms. Since hydrolysis is often considered the rate-limiting step in the anaerobic degradation of lignocellulosic biomass, this explains the observed alterations in degradation kinetics.

Table 5
Results of kinetic modelling of the anaerobic digestion of (DES treated) common reed. Kinetic parameters of the Modified Gompertz Model, the Transference Model, the Logistic Function Model, the First Order Kinetics and the Cone Model. P_0: maximum biogas yield of substrate ($mL_N\ g_{VS}^{-1}$), R_m: maximum bigas production rate ($mL_N\ g_{VS}^{-1}\ d^{-1}$), λ: lag phase (d), k_h: rate constant (d^{-1}), s: shape factor (–), R^2: coefficient of determination (–), $RMSE$: root mean square error ($mL_N\ g_{VS}^{-1}$).

Common reed											
T	°C	–	90	90	90	110	110	110	130	130	130
t	min	–	20	40	60	20	40	60	20	40	60
Modified Gompertz Model											
P_0	$mL_N\ g_{VS}^{-1}$	494.9	488.9	437.4	435.7	449.8	498.6	506.1	513.1	534.7	546.1
R_m	$mL_N\ g_{VS}^{-1}\ d^{-1}$	30.59	29.41	29.06	26.26	32.49	34.53	43.79	59.52	75.89	78.85
λ	d	−0.3	0.1	0.2	−0.5	0.4	0.4	1	1.5	1.8	1.7
R^2	–	0.99	0.988	0.984	0.981	0.987	0.985	0.99	0.984	0.988	0.989
$RMSE$	$mL_N\ g_{VS}^{-1}$	12.7	14.52	14.86	15.56	13.73	16.58	13.44	17.05	15.1	14.82
Transference Model											
P_0	$mL_N\ g_{VS}^{-1}$	506.3	502.9	448.8	446.3	460.6	511.5	517	524.2	545.2	556.3
R_m	$mL_N\ g_{VS}^{-1}\ d^{-1}$	51.69	48.03	47.01	44.78	51.61	55	65.9	79.05	91.82	96.63
λ	d	0.5	0.8	0.8	0.6	0.8	0.8	0.9	0.9	0.9	0.8
R^2	–	0.998	0.996	0.993	0.995	0.992	0.991	0.988	0.974	0.966	0.967
$RMSE$	$mL_N\ g_{VS}^{-1}$	6.56	8.96	10.09	8.41	10.91	12.64	15.1	21.75	25.44	25.16
Logistic Function Model											
P_0	$mL_N\ g_{VS}^{-1}$	490.4	483.8	433.3	431.6	445.9	494	502.5	509.9	532	543.5
R_m	$mL_N\ g_{VS}^{-1}\ d^{-1}$	28.68	27.86	27.59	24.42	31.11	33	42.36	59.83	76.8	79.88
λ	d	−0.5	0.1	0.2	−0.7	0.5	0.4	1.1	1.7	2.1	2
R^2	–	0.976	0.972	0.966	0.963	0.971	0.968	0.976	0.971	0.979	0.98
$RMSE$	$mL_N\ g_{VS}^{-1}$	19.48	21.63	21.03	21.51	19.81	23.41	20.03	22.03	19.46	19.15
First Order Kinetics											
P_0	$mL_N\ g_{VS}^{-1}$	509.2	507.8	452.8	449.2	464.3	515.9	520.9	527.6	548.3	559.1
k_h	d^{-1}	0.1	0.09	0.09	0.09	0.1	0.1	0.11	0.13	0.14	0.15
R^2	–	0.995	0.99	0.987	0.992	0.985	0.984	0.976	0.955	0.94	0.943
$RMSE$	$mL_N\ g_{VS}^{-1}$	8.99	12.81	13.25	10.13	14.24	16.2	19.73	26.07	30.37	30
Cone Model											
P_0	$mL_N\ g_{VS}^{-1}$	528.6	522	462.7	468.8	471.2	524.5	521.5	523.2	540.7	552.2
k_h	d^{-1}	0.13	0.12	0.13	0.13	0.14	0.13	0.15	0.18	0.19	0.2
s	–	1.6	1.7	1.8	1.6	1.9	1.8	2.1	2.4	2.8	2.8
R^2	–	1	0.999	0.998	0.998	0.999	0.998	0.999	0.994	0.994	0.995
$RMSE$	$mL_N\ g_{VS}^{-1}$	2.96	3.28	5.08	5.32	4.66	6.38	5.08	10.79	10.52	10.19

3.4. Comparison with conventional pre-treatment methods

Since DES is advertised as an alternative to conventional chemical pre-treatment methods, it is essential to assess its effectiveness in relation to other conventional methods such as acid and alkaline pre-treatment. As far as the effectiveness of the treatment is concerned, alkaline pre-treatment, for example, can lead to a comparatively strong increase in biogas potential. This is due to its ability to disrupt lignin structures, to break linkages between lignin and carbohydrates, to depolymerize, and to reduce cellulose crystallinity [70]. Treatment with acid can lead to the disintegration of lignin as well. A major limitation of the method is the formation of inhibitors like furfural and HMF [70]. Also, it has a lower selectivity towards lignin than alkaline and DES pre-treatment, as cellulose degradation may occur. As a result, the biogas potential of the treated solid biomass residues is not necessarily increased [70]. This effect could be observed in a screening test series performed accompanying the present investigation. A comparison of an acid and alkaline pre-treatment was carried out with the same feedstock, i.e., common reed, used in the present study. The method description and results are presented in the supplementary (section S.1., Figure S.1). The results of the supplementary screening show that the acidic treatment led to a considerable reduction in the biogas potential. This loss was up to - 43 %, while the DES treatment under the same conditions (130 °C, 60 min) resulted in a plus of +21 %. The alkaline pre-treatment was more effective under the same conditions (+27 %) and similarly effective under milder pre-treatment conditions (+19 %, 90 °C, 60 min) compared to the DES treatment. All methods had a comparable mass loss and approximately the same solid recovery when pre-treating at 130 °C for 60 min, i.e., 57 % (acid), 53 % (alkaline), and 54 % (DES). Overall, DES appears to have not only the conceptual advantages in terms of sustainability mentioned in the introduction, but also to be a competitive alternative to conventional methods in terms of biogas potential.

4. Conclusion

The present study investigated the suitability of process residues as biogas substrate, which result from a biorefinery process employing DES treatment to valorize lignocellulosic biomasses. Three different biomass streams, namely cork dust, olive tree pruning, and common reed, underwent DES treatment (ChCl:FA, 1:2 M ratio, 1:10 (g mL^{1-}) SSR) at various conditions.

While the extent of the effect varies across different biomasses, a significant increase in biogas and methane potential and altered degradation kinetics were observed. Specifically, the biogas yield increased by 125 % for cork dust, 21 % for olive tree pruning, and 12 % for common reed under treatment conditions of 130 °C for 60 min. Accordingly, the maximum biogas production rate (R_m) and rate constants (k, k_h) increased with treatment severity. The enhancement was attributed to the retention of the fermentable glucan fraction in the solid biomass, while hemicellulose and lignin tend to solubilize in the solvent. Lignin deformation and changes in crystallinity were also visible in the FTIR spectra. Taking solid recovery into consideration, the aforementioned increase in biogas reduces considerably. At worst, this means that substantially less biogas can be produced from the initial amount of biomass. Nevertheless, there remains an advantage of effect demonstrated here, namely a higher specific biogas yield and faster degradation of the treated samples compared to the respective untreated raw materials.

It should be considered that this study is limited by the number of biomass types and pre-treatment conditions investigated, which may not fully capture the diversity of real-world applications. For instance, further research could focus on the comparison of different DES. Additionally, the analysis is restricted to the solid phase, excluding possible liquid phase valorization pathways. Overall, the discussion shows that employing DES solely for pre-treating biogas substrates alone is questionable. Moreover, the use of chemicals and energy for pre-treatment should be factored into a holistic evaluation of the process. Nonetheless, integration into a biorefinery process, including a valorization step, is a conceivable sustainable application of deep eutectic solvents. Given that research in this area is still evolving, processes should be developed to satisfy sustainable and economic considerations. Techno-economic assessments and life cycle assessments are essential for scientifically evaluating the feasibility and environmental impact of DES applications, ensuring their alignment with both economic viability and sustainability goals.

CRediT authorship contribution statement

Jana Schultz: Writing – original draft, Visualization, Software, Methodology, Investigation, Formal analysis, Conceptualization. **Asli Isci:** Writing – review & editing, Methodology, Investigation, Formal analysis. **Marvin Scherzinger:** Writing – review & editing, Methodology, Formal analysis, Conceptualization. **Simel Bagder Elmaci:** Writing – review & editing, Methodology, Investigation. **Miyase Deniz Cam:** Investigation. **Dicle Delal Aslanhan:** Investigation. **Ozge Sakiyan:** Investigation. **Martin Kaltschmitt:** Writing – review & editing, Supervision, Resources, Project administration, Funding acquisition.

Data availability

Data will be made available upon request.

Funding

The authors acknowledge the financial support for the work published by the German Federal Ministry of Education and Research (grant number: 02WPM1656) and The Scientific and Technological Research Council of Turkey (TÜBİTAK) (Project No: 122N048).

Declaration of competing interest

The authors declare the following financial interests/personal relationships which may be considered as potential competing interests:

Jana Schultz reports financial support was provided by Federal Ministry of Education and Research Berlin Office. Martin Kaltschmitt, Marvin Scherzinger reports financial support was provided by Federal Ministry of Education and Research Berlin Office. Asli Isci, Simel Bagder Elmaci, Miyase Deniz Cam, Dicle Delal Aslanhan, Ozge Sakiyan reports financial support was provided by Scientific and Technological Research Council of Turkey. If there are other authors, they declare that they have no known competing financial interests or personal relationships that could have appeared to influence the work reported in this paper.

Acknowledgements

This research is part of the international research project ReMediation (Resilient Mediterranean with a holistic approach to sustainable agriculture: Addressing challenges of water, soil, energy and biodiversity; https://remediationproject.com/) within the PRIMA program (https://prima-med.org/).

Appendix A. Supplementary data

Supplementary data to this article can be found online at https://doi.org/10.1016/j.renene.2025.123215.

References

[1] L. Andersen, A. Lamp, C. Dieckmann, S. Baetge, L.-M. Schmidt, M. Kaltschmitt, Biogas plants as key units of biorefinery concepts: options and their assessment, J. Biotechnol. 283 (2018) 130–139, https://doi.org/10.1016/j.jbiotec.2018.07.041.
[2] Y. Zhou, D. Swidler, S. Searle, C. Baldino, Life-cycle greenhouse gas emissions of biomethane and hydrogen pathways in the European Union. https://theicct.org/wp-content/uploads/2021/12/lca-biomethane-hydrogen-eu-oct21.pdf, 2021.
[3] S. Menegat, A. Ledo, R. Tirado, Greenhouse gas emissions from global production and use of nitrogen synthetic fertilisers in agriculture, Sci. Rep. 12 (2022) 14490, https://doi.org/10.1038/s41598-022-18773-w.
[4] T.D. Searchinger, O. James, P. Dumas, T. Kstner, S. Wirsenius, EU climate plan boosts bioenergy but sacrifices carbon storage and biodiversity, Nature 612 (2022) 27–30, https://doi.org/10.1038/d41586-022-04133-1.
[5] EBA, Statistical report 2023: tracking biogas and biomethane deployment across Europe. https://www.europeanbiogas.eu/eba-statistical-report-2023/, 2023.
[6] P. Li, C. Yang, Z. Jiang, Y. Jin, W. Wu, Lignocellulose pretreatment by deep eutectic solvents and related technologies: a review, J. Bioresour. Bioprod. 8 (2023) 33–44, https://doi.org/10.1016/j.jobab.2022.11.004.
[7] T. Xiao, M. Hou, X. Guo, X. Cao, C. Li, Q. Zhang, W. Jia, Y. Sun, Y. Guo, H. Shi, Recent progress in deep eutectic solvent(DES) fractionation of lignocellulosic components : a review, Renew. Sustain. Energy Rev. 192 (2024) 114243, https://doi.org/10.1016/j.rser.2023.114243.
[8] S.B. Elmaci, J. Schultz, A. Isci, M. Scherzinger, D.D. Aslanhan, M.D. Cam, O. Sakiyan, M. Kaltschmitt, Deep eutectic solvent pretreatment of cork dust - effects on biomass composition, phenolic extraction and anaerobic degradability, Waste Manag. 181 (2024) 114–127, https://doi.org/10.1016/j.wasman.2024.04.007.
[9] A.P. Abbott, G. Capper, D.L. Davies, R.K. Rasheed, V. Tambyrajah, Novel solvent properties of choline chloride/urea mixtures, Chem. Commun. (2003) 70–71, https://doi.org/10.1039/B210714G.
[10] A. Pandey, Bhawna, D. Dhingra, S. Pandey, Hydrogen bond donor/acceptor cosolvent-modified choline chloride-based deep eutectic solvents, J. Phys. Chem. B 121 (2017) 4202–4212, https://doi.org/10.1021/acs.jpcb.7b01724.
[11] X. Kang, C. Deng, R. Shinde, R. Lin, J.D. Murphy, Renewable deep eutectic solvents pretreatment improved the efficiency of anaerobic digestion by lignin extraction from willow, Energy Convers. Manag. 288 (2023) 117115, https://doi.org/10.1016/j.enconman.2023.117115.
[12] A. Satlewal, R. Agrawal, S. Bhagia, J. Sangoro, A.J. Ragauskas, Natural deep eutectic solvents for lignocellulosic biomass pretreatment: recent developments, challenges and novel opportunities, Biotechnol. Adv. 36 (2018) 2032–2050, https://doi.org/10.1016/j.biotechadv.2018.08.009.
[13] P. Di Profio, M. Ciulla, S. Di Giacomo, N. Barbacane, R.D. Wolicki, A. Fontana, S. Moffa, S. Pilato, G. Siani, Emerging green strategies for biogas upgrading through CO2 capture: from unconventional organic solvents to clathrate and semi-clathrate hydrates, J. Mol. Liq. 391 (2023) 123196, https://doi.org/10.1016/j.molliq.2023.123196.
[14] J. Afonso, A. Mezzetta, I.M. Marrucho, L. Guazzelli, History repeats itself again: will the mistakes of the past for ILs be repeated for DESs? From being considered ionic liquids to becoming their alternative: the unbalanced turn of deep eutectic solvents, Green Chem. 25 (2023) 59–105, https://doi.org/10.1039/D2GC03198A.
[15] Z. Tang, C. Wu, W. Tang, C. Ma, Y.-C. He, A novel cetyltrimethylammonium bromide-based deep eutectic solvent pretreatment of rice husk to efficiently enhance its enzymatic hydrolysis, Bioresour. Technol. 376 (2023) 128806, https://doi.org/10.1016/j.biortech.2023.128806.
[16] Z. Sun, B. Fridrich, A. de Santi, S. Elangovan, K. Barta, Bright side of lignin depolymerization: toward new platform chemicals, Chem. Rev. 118 (2018) 614–678, https://doi.org/10.1021/acs.chemrev.7b00588.
[17] M.A. Alam, G. Muhammad, M.N. Khan, M. Mofijur, Y. Lv, W. Xiong, J. Xu, Choline chloride-based deep eutectic solvents as green extractants for the isolation of phenolic compounds from biomass, J. Clean. Prod. 309 (2021) 127445, https://doi.org/10.1016/j.jclepro.2021.127445.
[18] G.-C. Xu, J.-C. Ding, R.-Z. Han, J.-J. Dong, Y. Ni, Enhancing cellulose accessibility of corn stover by deep eutectic solvent pretreatment for butanol fermentation, Bioresour. Technol. 203 (2016) 364–369, https://doi.org/10.1016/j.biortech.2015.11.002.
[19] A. Isci, N. Thieme, A. Lamp, V. Zverlov, M. Kaltschmitt, Production of xylo-oligosaccharides from wheat straw using microwave assisted deep eutectic solvent pretreatment, Ind. Crop. Prod. 164 (2021) 113393, https://doi.org/10.1016/j.indcrop.2021.113393.
[20] DIN, Solid Biofuels – Determination of Moisture Content. DIN EN ISO 18134, Deutsches Institut für Normung e. V., 2015.
[21] Sludge Din, Treated biowaste, soil and waste - sludge, sludge, treated biowaste, soil and waste - determination of loss on ignition loss on ignitio. DIN EN 15935, Deutsches Institut für Normung e. V., 2012.
[22] A. Sluiter, B. Hames, R. Ruiz, C. Scarlata, J. Sluiter, D. Templeton, D. Crocker, Determination of Structural Carbohydrates and Lignin in Biomass: Laboratory Analytical Procedure (LAP), 2008.

[23] M.L. Nelson, R.T. O'Connor, Relation of certain intrared bands to cellulose crystallinity and crystal lattice type. part II. A new infrared ratio for estimation of crystallinity in cellulose I and II, J. Appl. Polym. Sci. 8 (1964) 1325–1341.
[24] J.G. Lynam, N. Kumar, M.J. Wong, Deep eutectic solvents' ability to solubilize lignin, cellulose, and hemicellulose; thermal stability; and density, Bioresour. Technol. 238 (2017) 684–689, https://doi.org/10.1016/j.biortech.2017.04.079.
[25] J. Shi, J. Li, Metabolites and chemical changes in the wood-forming tissue of Pinus koraiensis under inclined conditions, Bioresources 7 (2012) 3463–3475.
[26] W. Fang, n. Weisheng, Z. Andong, Y. Weiming, Enhanced anaerobic digestion of corn stover by thermo-chemical pretreatment, Int. J. Agric. Biol. Eng. 8 (2015) 84–90, https://doi.org/10.3965/j.ijabe.20150801.011.
[27] Verein Deutscher Ingenieure, Fermentation of Organic Materials - Characterisation of the Substrate, Sampling, Collection of Material Data, Fermentation Tests, 13.030.30, 27.190, 2016.
[28] D. Sonntag, D. Heinze, Sättigungsdampfdruck- Und Sättigungsdampfdichtetafeln Für Wasser Und Eis, 1. Edition, Deutscher Verlag für Grundstoffindurstrie, 1982.
[29] S. Meraj, R. Liaquat, S. Raza Naqvi, Z. Sheikh, A. Zainab, A.H. Khoja, D. Juchelkova, A. Atabani, Enhanced methane production from anaerobic Co-Digestion of wheat straw rice straw and sugarcane bagasse: a kinetic analysis, Appl. Sci. 11 (2021) 6069, https://doi.org/10.3390/app11136069.
[30] Z. Zahan, M.Z. Othman, T.H. Muster, Anaerobic digestion/co-digestion kinetic potentials of different agro-industrial wastes: a comparative batch study for C/N optimisation, Waste Manag. 71 (2018) 663–674, https://doi.org/10.1016/j.wasman.2017.08.014.
[31] H. Pereira, Variability of the chemical composition of Cork, Bioresources 8 (2013), https://doi.org/10.15376/biores.8.2.2246-2256.
[32] M. Cunha, A. Lourenço, S. Barreiros, A. Paiva, P. Simões, Valorization of Cork using subcritical water, Molecules 25 (2020), https://doi.org/10.3390/molecules25204695.
[33] P.C.R.O. Pinto, A.F. Sousa, A.J.D. Silvestre, C.P. Neto, A. Gandini, C. Eckerman, B. Holmbom, Quercus suber and Betula pendula outer barks as renewable sources of oleochemicals: a comparative study, Ind. Crop. Prod. 29 (2009) 126–132, https://doi.org/10.1016/j.indcrop.2008.04.015.
[34] J.B. Engel, C.L. Luchese, I.C. Tessaro, Characterization techniques comparison towards a better understanding of different cork-based stoppers types, J. Food Eng. 328 (2022) 111063, https://doi.org/10.1016/j.jfoodeng.2022.111063.
[35] J.F. García Martín, M. Cuevas, C.-H. Feng, P. Álvarez Mateos, M. Torres García, S. Sánchez, Energetic valorisation of olive biomass: olive-tree pruning, olive stones and pomaces, Processes 8 (2020) 511, https://doi.org/10.3390/pr8050511.
[36] J. Lizasoain, M. Rincón, F. Theuretzbacher, R. Enguídanos, P.J. Nielsen, A. Potthast, T. Zweckmair, A. Gronauer, A. Bauer, Biogas production from reed biomass: effect of pretreatment using different steam explosion conditions, Biomass Bioenergy 95 (2016) 84–91, https://doi.org/10.1016/j.biombioe.2016.09.021.
[37] M. Scherzinger, M. Kaltschmitt, M. Thoma, Effects of vapothermal pretreatment on anaerobic degradability of common reed, Energy Technol. 9 (2021), https://doi.org/10.1002/ente.202001046.
[38] Y.T. Tan, A.S.M. Chua, G.C. Ngoh, Deep eutectic solvent for lignocellulosic biomass fractionation and the subsequent conversion to bio-based products - a review, Bioresour. Technol. 297 (2020) 122522, https://doi.org/10.1016/j.biortech.2019.122522.
[39] Q. Yu, A. Zhang, W. Wang, L. Chen, R. Bai, X. Zhuang, Q. Wang, Z. Wang, Z. Yuan, Deep eutectic solvents from hemicellulose-derived acids for the cellulosic ethanol refining of Akebia' herbal residues, Bioresour. Technol. 247 (2018) 705–710, https://doi.org/10.1016/j.biortech.2017.09.159.
[40] Y.T. Tan, G.C. Ngoh, A.S.M. Chua, Effect of functional groups in acid constituent of deep eutectic solvent for extraction of reactive lignin, Bioresour. Technol. 281 (2019) 359–366, https://doi.org/10.1016/j.biortech.2019.02.010.
[41] W. Wang, D.-J. Lee, Lignocellulosic biomass pretreatment by deep eutectic solvents on lignin extraction and saccharification enhancement: a review, Bioresour. Technol. 339 (2021) 125587, https://doi.org/10.1016/j.biortech.2021.125587.
[42] Y.-L. Loow, E.K. New, G.H. Yang, L.Y. Ang, L.Y.W. Foo, T.Y. Wu, Potential use of deep eutectic solvents to facilitate lignocellulosic biomass utilization and conversion, Cellulose 24 (2017) 3591–3618, https://doi.org/10.1007/s10570-017-1358-y.
[43] Y.-L. Loow, T.Y. Wu, G.H. Yang, L.Y. Ang, E.K. New, L.F. Siow, J. Md Jahim, A. W. Mohammad, W.H. Teoh, Deep eutectic solvent and inorganic salt pretreatment of lignocellulosic biomass for improving xylose recovery, Bioresour. Technol. 249 (2018) 818–825, https://doi.org/10.1016/j.biortech.2017.07.165.
[44] A. Isci, G.M. Erdem, S. Bagder Elmaci, O. Sakiyan, A. Lamp, M. Kaltschmitt, Effect of microwave-assisted deep eutectic solvent pretreatment on lignocellulosic structure and bioconversion of wheat straw, Cellulose 27 (2020) 8949–8962, https://doi.org/10.1007/s10570-020-03371-8.
[45] B.J. Poddar, S.P. Nakhate, R.K. Gupta, A.R. Chavan, A.K. Singh, A.A. Khardenavis, H.J. Purohit, A comprehensive review on the pretreatment of lignocellulosic wastes for improved biogas production by anaerobic digestion, Int. J. Environ. Sci. Technol. 19 (2022) 3429–3456, https://doi.org/10.1007/s13762-021-03248-8.
[46] L. Li, X. Zhang, R. Che, M. Zhang, F. Xu, Pretreatment with ChOH/Urea under mild conditions for the efficient deconstruction of poplar cell wall, Ind. Crop. Prod. 204 (2023) 117316, https://doi.org/10.1016/j.indcrop.2023.117316.
[47] V.Z. Ong, T.Y. Wu, C.B.T.L. Lee, N.W.R. Cheong, K.P.Y. Shak, Sequential ultrasonication and deep eutectic solvent pretreatment to remove lignin and recover xylose from oil palm fronds, Ultrason. Sonochem. 58 (2019) 104598, https://doi.org/10.1016/j.ultsonch.2019.05.015.
[48] X. Li, W. Tang, Y.-C. He, Integrated understanding of acidic deep eutectic solvent choline chloride: oxalic acid pretreatment to enhance the enzymatic hydrolysis of rape straw, Ind. Crop. Prod. 206 (2023) 117691, https://doi.org/10.1016/j.indcrop.2023.117691.
[49] H. Li, J. Liang, F. Kong, M. Ren, A.E.A. Yagoub Mohammed, C. Zhou, Preparation of lignin-containing cellulose nanofibers from walnut shell using deep eutectic solvent for nanotube conductive film, Ind. Crop. Prod. 207 (2024) 117737, https://doi.org/10.1016/j.indcrop.2023.117737.
[50] L. Zhang, C. Zhang, Y. Ma, X. Zhao, X. Zhang, Lignocellulose pretreatment by deep eutectic solvent and water binary system for enhancement of lignin extraction and cellulose saccharification, Ind. Crop. Prod. 211 (2024) 118257, https://doi.org/10.1016/j.indcrop.2024.118257.
[51] M. Zhou, M. Lv, S. Cai, X. Tian, Effects of enzymatic hydrolysis and physicochemical properties of lignocellulose waste through different choline based deep eutectic solvents (DESs) pretreatment, Ind. Crop. Prod. 195 (2023) 116435, https://doi.org/10.1016/j.indcrop.2023.116435.
[52] M.H. Lopes, C.P. Neto, A.S. Barros, D. Rutledge, I. Delgadillo, A.M. Gil, Quantitation of aliphatic suberin in *Quercus suber* L. cork by FTIR spectroscopy and solid-state[13] C-NMR spectroscopy, Biopolymers 57 (2000) 344–351, https://doi.org/10.1002/1097-0282(2000)57:6<344::AID-BIP40>3.0.CO;2.
[53] C. Pascoal Neto, J. Rocha, A. Gil, N. Cordeiro, A.P. Esculcas, S. Rocha, I. Delgadillo, J.D. de Jesus, A.J. Correia, 13C solid-state nuclear magnetic resonance and fourier transform infrared studies of the thermal decomposition of cork, Solid State Nucl. Magn. Reson. 4 (1995) 143–151, https://doi.org/10.1016/0926-2040(94)00039-F.
[54] F. Xu, J. Yu, T. Tesso, F. Dowell, D. Wang, Qualitative and quantitative analysis of lignocellulosic biomass using infrared techniques: a mini-review, Appl. Energy 104 (2013) 801–809, https://doi.org/10.1016/j.apenergy.2012.12.019.
[55] S.M. Rocha, B.J. Goodfellow, I. Delgadillo, C.P. Neto, A.M. Gil, Enzymatic isolation and structural characterisation of polymeric suberin of cork from Quercus suber L, Int. J. Biol. Macromol. 28 (2001) 107–119, https://doi.org/10.1016/S0141-8130(00)00163-X.
[56] H. Garcia, R. Ferreira, M. Petkovic, J.L. Ferguson, M.C. Leitão, H.Q.N. Gunaratne, K.R. Seddon, L.P.N. Rebelo, C. Silva Pereira, Dissolution of cork biopolymers in biocompatible ionic liquids, Green Chem. 12 (2010) 367, https://doi.org/10.1039/b922553f.
[57] J.I. Santos, R. Martín-Sampedro, Ú. Fillat, J.M. Oliva, M.J. Negro, M. Ballesteros, M.E. Eugenio, D. Ibarra, Evaluating lignin-rich residues from biochemical ethanol production of wheat straw and olive tree pruning by FTIR and 2D-NMR, Int. J. Polym. Sci. 2015 (2015) 1–11, https://doi.org/10.1155/2015/314891.
[58] D. Ibarra, J.C. del Río, A. Gutiérrez, I.M. Rodríguez, J. Romero, M.J. Martínez, Á. T. Martínez, Isolation of high-purity residual lignins from eucalypt paper pulps by cellulase and proteinase treatments followed by solvent extraction, Enzym. Microb. Technol. 35 (2004) 173–181, https://doi.org/10.1016/j.enzmictec.2004.04.002.
[59] R. Mota-Panizio, M.J. Hermoso-Orzáez, L. Carmo-Calado, G. Lourinho, P.S.D. de Brito, Biochemical methane potential of Cork boiling wastewater at different inoculum to substrate ratios, Appl. Sci. 11 (2021) 3064, https://doi.org/10.3390/app11073064.
[60] R. Guan, H. Yuan, S. Yuan, B. Yan, X. Zuo, X. Chen, X. Li, Current development and perspectives of anaerobic bioconversion of crop stalks to biogas: a review, Bioresour. Technol. 349 (2022) 126615, https://doi.org/10.1016/j.biortech.2021.126615.
[61] C. Nitsos, L. Matsakas, K. Triantafyllidis, U. Rova, P. Christakopoulos, Evaluation of Mediterranean agricultural residues as a potential feedstock for the production of biogas via anaerobic fermentation, BioMed Res. Int. 2015 (2015) 171635, https://doi.org/10.1155/2015/171635.
[62] L. Bianchini, P. Costa, P.P. Dell'Omo, A. Colantoni, M. Cecchini, D. Monarca, An industrial scale, mechanical process for improving pellet quality and biogas production from hazelnut and olive pruning, Energies 14 (2021) 1600, https://doi.org/10.3390/en14061600.
[63] S. Vakalis, A. Georgiou, K. Moustakas, M. Fountoulakis, Assessing the effect of hydrothermal treatment on the volatile solids content and the biomethane potential of common reed (Phragmites australis), Bioresour. Technol. Rep. 17 (2022) 100923, https://doi.org/10.1016/j.biteb.2021.100923.
[64] C.A. Pizarro-Loaiza, P. Torres-Lozada, J. Illa, J. Palatsi, A. Bonmatí, Effect of harvesting Age and size reduction in the performance of anaerobic digestion of pennisetum grass, Processes 8 (2020) 1414, https://doi.org/10.3390/pr8111414.
[65] A.D. Olugbemide, A. Oberlintner, U. Novak, B. Likozar, Lignocellulosic corn stover biomass pre-treatment by Deep Eutectic Solvents (DES) for biomethane production process by bioresource anaerobic digestion, Sustainability 13 (2021) 10504, https://doi.org/10.3390/su131910504.
[66] H. Sha, S. Cao, B. Zhao, Z. Dong, G. Wang, J. Duan, Effect of alkaline deep eutectic solvents pretreatment on CH4 yield from anaerobic digestion of corn stover, Energy 302 (2024) 131683, https://doi.org/10.1016/j.energy.2024.131683.
[67] A. Nawaz, R. Chaudhary, I.U. Haq, X. Fu, R. Huang, H. Mukhtar, K. Jiang, Delignification of halophyte Atriplex crassifolia by green recyclable deep eutectic

solvents for enhanced production of biogas, Fermentation 9 (2023) 314, https://doi.org/10.3390/fermentation9030314.
[68] K. Kohli, S. Katuwal, A. Biswas, B.K. Sharma, Effective delignification of lignocellulosic biomass by microwave assisted deep eutectic solvents, Bioresour. Technol. 303 (2020) 122897, https://doi.org/10.1016/j.biortech.2020.122897.
[69] S. Park, J.O. Baker, M.E. Himmel, P.A. Parilla, D.K. Johnson, Cellulose crystallinity index: measurement techniques and their impact on interpreting cellulase performance, Biotechnol. Biofuels 3 (2010). http://www.biotechnologyforbiofuels.com/content/3/1/10.
[70] S. Behera, R. Arora, N. Nandhagopal, S. Kumar, Importance of chemical pretreatment for bioconversion of lignocellulosic biomass, Renew. Sustain. Energy Rev. 36 (2014) 91–106, https://doi.org/10.1016/j.rser.2014.04.047.
[71] M. Scherzinger, M. Kaltschmitt, A.Y. Elbanhawy, Anaerobic biogas formation from crops' agricultural residues - modeling investigations, Bioresour. Technol. 359 (2022) 127497, https://doi.org/10.1016/j.biortech.2022.127497.